

## Causality in heliophysics: Magnetic fields as a bridge between the Sun's interior and the Earth's space environment

Dibyendu Nandy <sup>a,b,\*</sup>, Yoshita Baruah <sup>a,b</sup>, Prantika Bhowmik <sup>c</sup>, Soumyaranjan Dash <sup>a</sup>,  
Sakshi Gupta <sup>a,b</sup>, Soumitra Hazra <sup>d</sup>, B. Lekshmi <sup>e</sup>, Sanchita Pal <sup>f,g</sup>, Shaonwita Pal <sup>a</sup>, Souvik Roy <sup>a</sup>,  
Chitradeep Saha <sup>a</sup>, Suvidip Sinha <sup>a</sup>

<sup>a</sup> Center of Excellence in Space Sciences, India, Indian Institute of Science Education and Research Kolkata, Mohanpur, 741246, West Bengal, India

<sup>b</sup> Department of Physical Sciences, Indian Institute of Science Education and Research Kolkata, Mohanpur, 741246, West Bengal, India

<sup>c</sup> Department of Mathematical Sciences, Durham University, Durham, DH1 3LE, UK

<sup>d</sup> Lowell Center for Space Science and Technology, University of Massachusetts Lowell, 600 Suffolk Street, Lowell, 01854, MA, USA

<sup>e</sup> Max Planck Institute for Solar System Research, Göttingen, D-37077, Germany

<sup>f</sup> Heliophysics Science Division, NASA Goddard Space Flight Center, 8800 Greenbelt Road, Greenbelt, 20771, MD, USA

<sup>g</sup> Department of Physics and Astronomy, George Mason University, Fairfax, 22030, VA, USA



### ARTICLE INFO

#### Keywords:

Sun  
Earth  
Heliosphere

### ABSTRACT

Our host star, the Sun, is a middle-aged main sequence G type star whose activity varies. These variations are primarily governed by solar magnetic fields which are produced in the Sun's interior via a magnetohydrodynamic dynamo mechanism. Solar activity manifests across different timescales, spanning transient phenomena such as flares, energetic particle events and coronal mass ejections to short to long-term modulation of solar irradiance, plasma winds, open flux and cosmic ray flux in the heliosphere. Collectively, these phenomena define space weather and space climate, which impact the state of the near-Earth space environment, the Earth's magnetosphere, atmosphere and our space-reliant technologies. Understanding physical processes that are at the heart of solar variability and which causally connect the Sun–Earth system is therefore of immense importance to humanity. Such understanding leads to predictions of the impact of solar activity on our planet and provides a window to explore the plasma universe and other star–planet systems, including assessing the habitability of (exo)planets. In this review, based on our research on the solar–terrestrial system and extant scientific literature, we illuminate processes related to the genesis of solar magnetic fields in the Sun's interior, their emergence and evolution, their manifestation as solar eruptive events, and their eventual impact on the geospace environment mediated via solar winds and storms. We focus on few phenomena that establish causal connections and demonstrate how our current understanding can lead to development of predictive capabilities encompassing the domain of heliophysics.

### 1. Introduction

Our home planet – the Earth – is a unique place that is inhabited by living beings, as known to humanity so far. Existence of life on Earth can largely be attributed to its host star, the Sun, which not only keeps the planet gravitationally bound to an orbit but also radiates energy output essential for the sustenance of life. The Sun is classified as a G2-type middle-aged main-sequence star with an age of 4.6 billion years, burning hydrogen at its core and churning plasma in its outer convective shell; to turn the star magnetically active. It is widely

accepted that there exists a dynamo mechanism driven by the plasma motion in the solar interior which periodically generates and recycles the magnetic fields in the Sun (Charbonneau, 2020; Hazra et al., 2023). The large-scale solar magnetic activity typically surges and ebbs over an 11-year timescale known as ‘solar cycle’ (Schwabe, 1844; Hathaway, 2015). On the other hand, long-term direct observations complemented by reconstructions based on cosmogenic radionuclide abundance reveal the presence of centennial to millennial time scale modulations in the activity of Sun (Usoskin, 2017).

\* Corresponding author at: Center of Excellence in Space Sciences, India, Indian Institute of Science Education and Research Kolkata, Mohanpur, 741246, West Bengal, India.

E-mail address: [dnandi@iiserkol.ac.in](mailto:dnandi@iiserkol.ac.in) (D. Nandy).

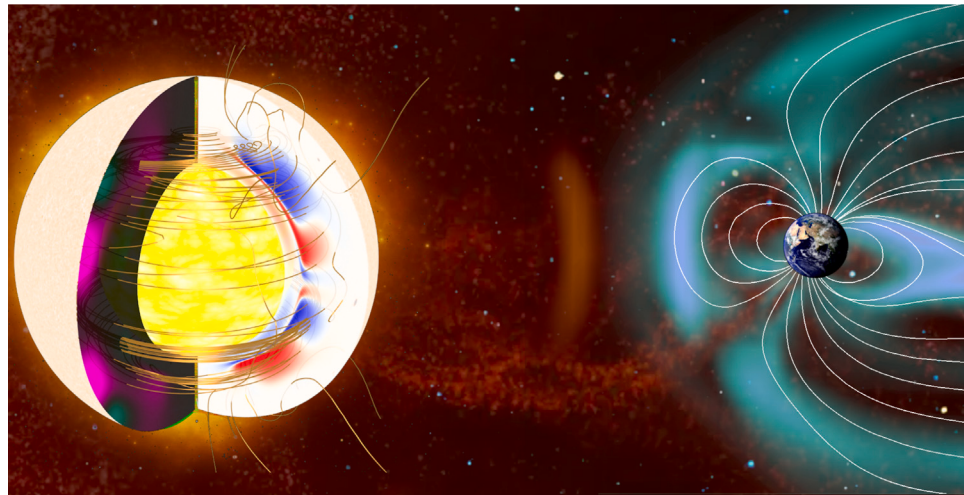


**Fig. 1.** An artist's impression of the heliospheric ecosystem with a modeled Sun on the left, and on the right the Earth (not to scale). Earth is gravitationally bound and magnetically linked to its host star – the Sun. Variation of magnetic activity in the solar interior eventually regulates the Earth's magnetosphere-atmosphere across timescales ranging from transitory to evolutionary. Solar dynamo visualization by NASA/GoddardSpaceFlightCenterScientificVisualizationStudio; based on (Muñoz-Jaramillo et al., 2009).

Turbulent plasma motions pervading the solar interior up to the surface give rise to complex structures of the solar magnetic field which can be found on scales as small as a few tens of kilometers, about the size of individual convective granules, to large active regions that can be more than a few thousand kilometers across. Strength of the global magnetic field of the Sun is approximately a few tens of Gauss, however, the magnetic field distribution in the Sun being in-homogeneous, in smaller spatial scales like the sunspots or bipolar magnetic regions – dark, magnetized regions on the solar surface – the solar magnetic field strength can reach up to several kilo Gauss (Hale, 1913). The field structures extend out to solar chromosphere and corona above the active regions, often reaching heights of several million kilometers. A near-consensus now exists that these active regions originate from a strong toroidal magnetic field stored at the base of the solar convection zone, generated by a deep-seated solar dynamo mechanism (Nandy and Choudhuri, 2002; Hathaway et al., 2003). Sunspots have transient internal fields that get advected as well as diffused due to the inductive action of plasma motions, on timescales ranging from days to months (Babcock, 1961). Such fields are entirely responsible for the thermal and dynamical structuring of the solar corona (Schrijver and DeRosa, 2003; Cook et al., 2009; Mackay and Yeates, 2012; Nandy et al., 2018). The bipolar magnetic regions are the seats of solar flares which are sporadic and massive explosions. Solar flares also often occur from complex multipolar magnetic configurations formed by the merging of different dipoles (Liu et al., 2021). They are sometimes associated with rapid eruptions of charged particles and radiations into space called coronal mass ejections, or CMEs (Wang and Zhang, 2007). Sufficiently strong Earth-directed CMEs have the potential to significantly perturb the Earth's magnetosphere and cause calamitous geomagnetic storms.

The magnetic influence of the Sun permeates through the entire solar system in the form of interplanetary magnetic field threaded by the ever-present solar wind; protecting the solar system from interstellar radiation, like a magnetized cocoon – called ‘heliosphere’ (see Fig. 1). While short-term, transient events such as solar flares and coronal mass ejections interact with Earth's magnetosphere, lit up the polar skies with cosmic fireworks called aurora, also pose tremendous hazards to the near-Earth space environmental conditions including Earth-orbiting satellites and other space-reliant technologies (Schrijver et al., 2015; Mursula et al., 2013), slower and long-term evolutions of solar activity result in variations in solar open flux, solar wind

properties, and recurrence of solar magnetic storms and thus eventually shape the planetary climate and habitability (Daglis et al., 2021; Nandy et al., 2021).

In the subsequent sections of this review, we revisit and celebrate the causal connections we share with the Sun – “one of a multitude, a single star among millions, yet near enough to affect terrestrial affairs to any sensible degree” (Young, 1896). No doubt, this review is not all encompassing of the field of heliophysics and solar–terrestrial connections, and is colored by our own research experiences and expertise. However, herein, we strive to give a flavor of the field by discussing specific phenomena that illuminate causal connections between the Sun–Earth system mediated via solar magnetic fields and their variability.

## 2. Solar magnetic field dynamics and its evolution

Ancient records of sunspot numbers and auroral activity (Lee et al., 2004) and, telescopic observation in the modern era (Wolf, 1852) show that the number of sunspots observed on the Sun rises and falls cyclically with a mean periodicity of eleven years, also known as the solar cycle (see Fig. 2, panel a). Besides, a closer inspection reveals dispersion in the solar cycle duration and more prominently, large fluctuations in the cycle amplitudes. Extreme behavior in solar activity has been observed at the time of grand minima when the number of sunspots on the solar surface remain remarkably low over several decades, and also at the time of grand maxima when the cycle amplitudes are larger than usual. Cosmogenic isotope-based solar activity reconstructions indicate multiple instances of grand solar minima in the past millennia – the most recent of which is known as the Maunder minimum (Eddy, 1976; Wu et al., 2018). Strikingly, the reconstructed long-term solar activity records also detect intervals devoid of grand minima (Vasiliev and Dergachev, 2002) and modulations in centennial to millennial timescale (Gleissberg, 1955; de Vries, 1958; Suess, 1965) – pointing toward a secular trend in the sunspot number time series. A surge in the number of solar flares and coronal mass ejection events is observed at the time of solar maximum. In summary, solar activity plays a vital role in shaping terrestrial and space climate conditions. However, accurate prediction of solar activity is an outstanding challenge due to such quasi-periodic irregular behavior of the solar cycle (Nandy, 2021).

In the next sub-sections, we discuss the interplay of plasma flows and magnetic fields in generating and sustaining variable solar–stellar

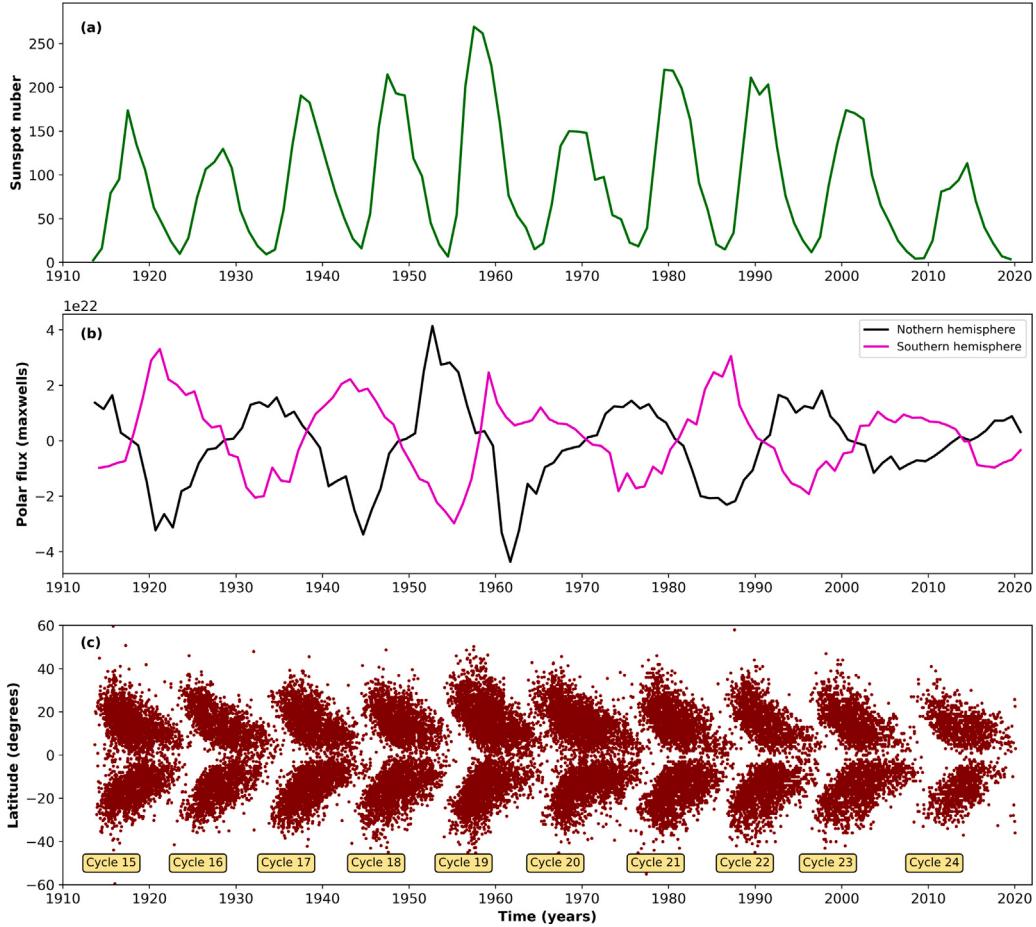


**Fig. 2.** Observed features of the solar cycle. (a) The sunspot time series is plotted from the year 1914.5 to 2019.5. The data is annually averaged (Clette et al., 2015) and obtained from the World Data Center, SILSO. It is well noticed that cycle amplitudes vary significantly. (b) Time series depicting the evolution of polar flux in both hemispheres is shown. This is the calibrated polar faculae data derived from the Mount Wilson Observatory and Wilcox Solar Observatory, and covers the period from 1914 to 2019.5 (Muñoz-Jaramillo et al., 2012). The magenta and black curves show the polar flux evolution in the southern and northern hemisphere respectively. One can find that either hemisphere has opposite polarity, generating the global dipole magnetic field of the Sun. (c) This is the sunspot butterfly diagram. This data is acquired from the Royal Greenwich Observatory/USAF-NOAA active region database and the Helioseismic and Magnetic Imager (HMI) instrument (Scherrer et al., 2012) for the period 1914 to 2019. The solar cycle numbers are specified in the bottom panel.

magnetic activity and its predictability, and recent progress in modeling and understanding the evolution of the solar magnetic field and the impact of solar forcing on the interplanetary medium.

### 2.1. Origin of solar magnetism: Solar dynamo mechanism

To understand the behavior of solar magnetic activity, it is necessary to understand the process of magnetic field generation in the Sun. Non-linear interaction between magnetic field and turbulent plasma flow inside the solar convection zone – known as dynamo mechanism – is believed to be responsible for generating large-scale solar magnetic fields. The primordial source of magnetic field in most of the newborn stars is the magnetic field existing in their parent molecular cloud core supplying matter and angular momentum to the protostars. This primordial field acts as a seed which can be amplified by the dynamo mechanism that involves conversion of kinetic energy in turbulent plasma flows to magnetic energy. Although fundamental magnetohydrodynamic equations are well established, modeling the turbulence in solar convection zone is crucial and this is where the mean field prescription of turbulence plays a vital role; for a recent review see Hazra et al. (2023).

In the mean-field prescription, the large-scale solar magnetic field is assumed to be axisymmetric and is decomposed into the toroidal (field in the longitudinal,  $\phi$ , direction) and poloidal (field in meridional planes) field. To explain the origin of the solar cycle, Parker (1955b)

proposed the idea of recycling between the toroidal and poloidal fields. Theoretical and numerical magnetoconvection studies indicate that magnetic field exists in the form of flux tubes inside the solar convection zone (Chandrasekhar, 1961; Proctor and Weiss, 1982). On the other hand, Alfvén (1942) showed that the magnetic fields tend to remain frozen in highly conductive plasma medium and move along with the plasma flow. As the Sun rotates differentially i.e., the solar equator rotates faster than the poles, the frozen-in poloidal component of the magnetic flux tubes get stretched along  $\phi$ -direction to induce a toroidal component – a process termed as  $\Omega$  effect (Parker, 1955a). This process is believed to be concentrated in a thin layer between solar radiative and convective zone – known as the tachocline – that hosts a very strong radial shear, as indicated by helioseismic observations. Sufficiently strong toroidal flux tubes generated near the tachocline can become unstable due to magnetic buoyancy and erupt radially outwards and eventually produce sunspots. The Coriolis force arising due to the rotation of the Sun imparts a vortical motion to the toroidal flux tubes rising through the convection zone. Thus sunspots appear as bipolar pairs with a systematic tilt relative to the local East–West direction. Joy's law describes the latitude dependence of the tilt of bipolar sunspot regions: the leading spots are closer to the equator than the following spots and this tilt angle increases with increasing latitude (Hale et al., 1919). The turbulent buffeting of the buoyant magnetic flux tubes rising through the solar convection zone adds a random component to the tilt of sunspots, contributing to dispersion

in the tilt angle distribution. Various kinds of stochastic forcing are introduced into numerical solar dynamo models to mimic this turbulent buffeting and to simulate intermittent behavior of the solar cycle – which will be further discussed in Section 2.4.

Conversion of toroidal field to the poloidal field in the Sun is a highly debated issue. Parker (1955b) suggested that helical, turbulent convection in the rotating systems – like the Sun – can twist the upward rising toroidal flux tubes to generate the poloidal field; known as the mean-field  $\alpha$ -effect. However, numerical flux tube simulations indicate that only those flux tubes with initial field strength of 50–100 kG, ten times higher than the equipartition field strength, are consistent with the observed tilt and emergence latitude of active regions (D'Silva and Choudhuri, 1993; Fan et al., 1993). At this strong field strength, it is impossible for helical convective turbulence to impart significant twists as required by the classical mean-field  $\alpha$ -effect. This realization led the dynamo research community to adopt an alternative proposal put forward by Babcock (1961) and Leighton (1969). They suggest that the evolution of bipolar sunspot pairs on the solar surface is subject to near-surface plasma flows – such as differential rotation, meridional circulation, and supergranular diffusion – which eventually contribute to equatorward (and poleward) migration of preceding (and following) polarity, resulting in the decay and dispersal of the associated magnetic flux. This process can regenerate the poloidal field at the surface; widely known as the Babcock–Leighton (BL) mechanism (Babcock, 1961; Leighton, 1969). The latter one is now believed to be the dominant process for driving solar cycle variations (Cameron and Schüssler, 2015; Bhowmik and Nandy, 2018).

Dynamo models imbuing the BL mechanism are called the flux-transport dynamo models (FT). In flux-transport dynamo models, the toroidal field is generated mainly at the base of the convection zone, while the poloidal field generation takes place near the solar surface. Communication between these two spatially separated regions is essential to obtain an operational dynamo. It is believed that turbulent diffusion, meridional circulation, and turbulent pumping play the role of communicator between these two source layers (Hazra and Nandy, 2016). Several physically inspired kinematic mean-field flux-transport solar dynamo models have been developed in the last decade which can successfully reproduce different observed solar cycle properties, such as cyclic reversal, the latitudinal distribution of sunspots, the observed phase relationship between the sunspot cycle and polar fields, etc (Durney, 1995; Dikpati and Charbonneau, 1999; Nandy and Choudhuri, 2001, 2002; Nandy, 2002; Guerrero and Munoz, 2004; Chatterjee et al., 2004; Guerrero and Dal Pino, 2008; Muñoz-Jaramillo et al., 2009; Muñoz-Jaramillo et al., 2010; Muñoz-Jaramillo et al., 2011; Nandy et al., 2011; Yeates and Muñoz-Jaramillo, 2013; Hazra and Nandy, 2016; Miesch and Teweldebirhan, 2016; Karak and Miesch, 2017; Kumar et al., 2019). However, self-consistent modeling of the complex, non-linear interactions between plasma flows and magnetic fields in the solar–stellar interior remains challenging. While full MHD, direct numerical simulations are yet to achieve realistic parameter regimes of stellar convection zones, significant advances have been made in capturing some of the characteristics of solar plasma flows, including cyclic behavior in solar–stellar magnetic activity (Brun et al., 2004; Ghizaru et al., 2010; Nelson et al., 2012; Hotta et al., 2016; Käpylä et al., 2017; Hotta et al., 2022). Recently, Hotta and Kusano (2021) have successfully reproduced solar-like differential rotation, convection, and magnetic field distribution in the solar convection zone using high-resolution full MHD simulations, which can provide better insights into the solar dynamo mechanism and also underscores the importance of exascale computational capabilities.

Since long-term simulations of solar magnetic activity using spatially extended numerical models are computationally expensive, there have been attempts to understand the secular trends and extreme solar activity episodes using spatially reduced kinematic dynamo models (Passos et al., 2014) and low-order dynamo models – some of which incorporate stochastic fluctuations in driving parameters of the solar

dynamo mechanism, non-linear feedback between convective plasma flows and magnetic fields (Knobloch et al., 1998; Wilmot-Smith et al., 2005; Weiss and Tobias, 2016), time-delay dynamics of the magnetic fields (Wilmot-Smith et al., 2006), or a combination of these effects (Hazra et al., 2014; Tripathi et al., 2021).

## 2.2. Transport properties inferred from helioseismic observations

As discussed in the previous section, solar magnetic activities are mostly direct consequences of the magnetic fields and the different types of plasma flow in the Sun's interior and surface. Observational constraints of the solar interior make it difficult to understand the magnetic field dynamics playing deep down in the solar convective zone that materializes in the photosphere and chromosphere of the Sun. However, Doppler imaging of the solar surface reveals the presence of five-minute oscillations of the solar surface (Leighton et al., 1962), resulting from the formation of standing acoustic waves in the solar interior. These acoustic waves are rich in information about the turbulent dynamics of the convective motions of the plasma blobs in the solar convection zone (Goldreich and Kumar, 1990). Here, the technique of *Helioseismology* (Gough et al., 1996) comes into play by aiding to utilize this rich reservoir of information (Hanasoge, 2022) to understand the dynamics of the solar interior.

Helioseismological observations made from space and ground-based observatories are designed to encapsulate the exquisite features on the solar surface and hence unravel the magnetic dynamics of the Sun. Global helioseismological techniques such as interpreting the eigenfrequencies of the resonant modes of oscillations (Christensen-Dalsgaard, 2002) shed light on the large-scale solar rotational features such as convective differential rotation. The methodology of global helioseismology, when combined with the promising local helioseismological techniques such as time–distance helioseismology (Duvall et al., 1993), direct modeling (Woodard, 2002), and ring-diagram analysis (Hill, 1999; Basu et al., 1999; Lekshmi et al., 2018, 2019) have helped us advance our theoretical understanding of the solar interior and the physics of the solar cycle.

The torsional oscillation and meridional flow in the solar interior obtained from global and local helioseismological studies primarily help us understand the dynamics in the solar convection zone. Additionally, the existence of these plasma flows also helps to understand the connection between the mass motions and large-scale magnetic features. The fluctuations in the mean differential rotation profile, the torsional oscillations, were first observed using full-disk velocity measurements from the Mount Wilson Observatory (Howard and Labonte, 1980). The evidence of torsional oscillations in the solar convective zone persists over a large fraction of the solar convection belt (Howe et al., 2000), and its properties vary with the latitudes. Lekshmi et al. (2018) show that the hemispherical asymmetry in near-surface torsional oscillation velocity is well correlated with the asymmetry in magnetic flux and sunspot number at the solar surface. It is speculated that the asymmetry in torsional oscillation may trigger the conventional north–south hemispherical asymmetry in the solar cycle (Gigolashvili et al., 2005; Lekshmi et al., 2018).

The existence of meridional flow from the equator to the poles was first characterized by surface Doppler measurements (Hathaway, 1996). But, measuring the meridional flow strength in the convection zone is challenging due to its weak strength compared to the differential rotation. Helioseismological techniques such as inversions constrained with mass conservation (Giles, 2000), time–distance helioseismology (Chou and Dai, 2001; Gizon et al., 2001; Zhao and Kosovichev, 2004), and ring diagram analyses (Basu et al., 1999; Haber et al., 2002) provide fairly consistent estimations of the near-surface meridional flow. Feature tracking and helioseismic measurements (Hathaway et al., 1996) reveal that the flow is directed poleward on the solar surface and has an amplitude of about 10 m/s to 15 m/s. Most of these measurements assume hemispherical symmetry of the

meridional flow to separate it from other larger flow components. The sophisticated tools of local helioseismology have further aided in delving into the fluctuations of the meridional circulation, which show them to be one of the ingredients governing north–south asymmetry seen in the sunspot cycle (Lekshmi et al., 2019).

Helioseismic studies are essential in probing plasma transportation and its characteristics on the near-surface layers and have been extremely important in studying the delicate structures and flows around the complex active regions (Braun, 2019), which further helps to understand the formation, maintenance and evolution of solar active regions.

### 2.3. Surface flux transport on a magnetic star: modeling the photospheric magnetic field

Surface flux transport on the Sun elucidates the solar-dynamo-driven process, in which the surface plasma flows carry the magnetic flux associated with the tilted active regions from the low latitudinal belts to the poles (Muñoz-Jaramillo et al., 2010; Jiang et al., 2014). Due to the incessant migration of the opposite leading polarity flux, the polar fields of the previous cycle get canceled during the solar maximum, and a new poloidal field of the opposite polarity begins to grow. The ultimate decay of sunspots and the generation of a newborn polar field is at the heart of the BL mechanism (Babcock, 1961; Hazra and Nandy, 2016; Kumar et al., 2019), mentioned in Section 2.1. Analytical and observational studies stipulate that the surface fields are the primary drivers of the internal dynamo (Cameron and Schüssler, 2015), and the strength of this newborn poloidal field during the solar minimum becomes the seed of the next solar cycle (Nandy, 2021). Thus it is pivotal to understand and model the spatio-temporal magnetic field evolution of the tilted magnetic sunspots on the solar surface. In this section, we portray the applicability and advancements in numerical modeling of surface flux transport on the solar surface by replicating the BL mechanism (well known as the ‘Surface Flux Transport Model’ or ‘SFT Model’) (Mackay and Yeates, 2012; Jiang et al., 2014). Observational evidence elucidates that the Sun’s photospheric magnetic field is primarily oriented along the radial direction (Solanki, 1993). Hence, the model emphasizes the solutions of the radial component of the induction equation driven by different kinds of large-scale transport profiles (Bhowmik and Nandy, 2018; Bhowmik, 2019; Dash et al., 2020b; Pal et al., 2023). The primary dynamical equation associated with the SFT model is,

$$\begin{aligned} \frac{\partial B_r}{\partial t} = & -\omega(\theta) \frac{\partial B_r}{\partial \phi} - \frac{1}{R_\odot \sin \theta} \frac{\partial}{\partial \theta} \left( v(\theta) B_r \sin \theta \right) \\ & + \frac{\eta}{R_\odot^2} \left[ \frac{1}{\sin \theta} \frac{\partial}{\partial \theta} \left( \sin \theta \frac{\partial B_r}{\partial \theta} \right) + \frac{1}{\sin^2 \theta} \frac{\partial^2 B_r}{\partial \phi^2} \right] \\ & + S(\theta, \phi, t). \end{aligned} \quad (1)$$

As discussed in Section 2.2, the advective meridional circulation ( $v(\theta)$ ) and differential rotation ( $\omega(\theta)$ ) can be modeled as a large-scale axisymmetric flow profile using mathematical equations inspired by observations (Snodgrass, 1983; van Ballegooijen et al., 1998). The random super-granular small-scale plasma flows can be mimicked by the magnetic diffusivity term ( $\eta$ ), provided the scales of interest are the size of an active region or higher. Diffusion helps in dispersing the magnetic flux associated with the sunspots throughout the solar surface isotropically. Lastly, the source term,  $S(\theta, \phi, t)$  in this SFT model Eq. (1) (Jiang et al., 2014; Bhowmik and Nandy, 2018; Pal et al., 2023) imitates the emergence of the sunspots on the surface that can be constructed in two ways: (1) Using data-driven mathematical modeling of the ideal bipolar magnetic region (Jiang et al., 2011; Bhowmik and Nandy, 2018), (2) Direct data assimilation of synoptic maps or SHARP data series (Yeates et al., 2015; Yeates, 2020).

The primary success of this type of dynamical models is to constrain the physical mechanism manifested in the observational findings. It can

also unravel some magnetic features which are not directly seen in the photospheric magnetogram. This model is designed to take input from the observational data of flux emergence to bring the results in agreement with the solar activity cycles. An example is portrayed in Fig. 3, which compares the observational and SFT simulated full disk magnetogram utilizing the spectral SFT code used in Nandy et al. (2018), Bhowmik and Nandy (2018), Bhowmik (2019), Dash et al. (2020a), Pal et al. (2023).

The observational butterfly diagram (time–latitudinal distribution of longitudinally averaged surface magnetic field) represents that the mid to higher-latitude fields are transported toward the poles, where they ultimately reverse the polar field at about the sunspot cycle maximum epoch (see panel (a) of Fig. 4). Data-driven SFT simulation (Bhowmik and Nandy, 2018) is also capable of reproducing the polar flux cancellation and build-up mechanism due to magnetic flux surges from mid-to-high latitudes during past solar cycles (see panel (b) of Fig. 4).

Another advantage of using an SFT model is its capability to provide full-Sun magnetograms, which are challenging to obtain from observation only. Firstly, since only one side of the Sun is visible at a time, the sunspots that emerge and decay on the far side are not observed. Secondly, the limb side data are often erroneous due to projection effects of the Sun. Thirdly, owing to the difficulty of observing the Sun’s poles, we lack polar magnetic field observation. All of these limiting factors result in some amount of missing (or erroneous) flux in observed magnetograms, which ultimately affects the simulations. In all cases, SFT simulations play an essential role in studying the long and short-term evolution of large-scale surface magnetic fields, including the polar fields (Petrie, 2015; Dash et al., 2020b; Nandy et al., 2023). Moreover, SFT models can be used as a crucial tool for solar cycle predictions and for modeling open magnetic flux using the available historical data, a detailed discussion on which follows in Section 2.4.

However, such numerical models can be improved further by incorporating more observational details where the focus is to investigate the short-term and small-scale evolution of the surface magnetic field. This requires the flow profiles of granular, super-granular convective inferred from observations and plasma inflows around active regions fitted in the SFT model, which is still in progress and has openings for future research in this field (Upton and Hathaway, 2013; Martin-Belda and Cameron, 2016).

Beyond the surface magnetic field evolution, the BL mechanism (captured through SFT simulations) govern the coronal magnetic field distribution, which is essential in discerning our space weather. In short, the evolution of the interior and surface fields of the interplanetary magnetic fields, solar winds, and coronal emissions, all of which influence the magnetic interactions of the Sun–Earth system. This knowledge can further be applied to any star–planet system, and their magnetic interactions can thus be investigated. The magnetic and energetic environment around an (exo)planet and its impact on the magnetospheric–atmospheric coupling are essential components of a planet’s habitability which we further expect to constrain the application of simulated stellar magnetic activity that will be discussed in detail in the next sections.

### 2.4. Simulating and predicting solar magnetic variability

The decadal scale variations observed on the Sun, i.e., the solar cycle output of magnetic fields, solar irradiance and energetic particles impact the Earth’s space environment and upper atmosphere; these are relevant for mission planning and mission life time estimates. Long-term variations impact space climate and atmospheric dynamics. Solar activity predictions are essential in this context. Approaches to forecast future solar cycle amplitudes are based on different techniques, which include precursor, model-based, statistical extrapolation techniques, and machine learning approaches (Petrovay, 2020; Nandy, 2021). Nevertheless, prediction of future cycle amplitudes remains challenging due

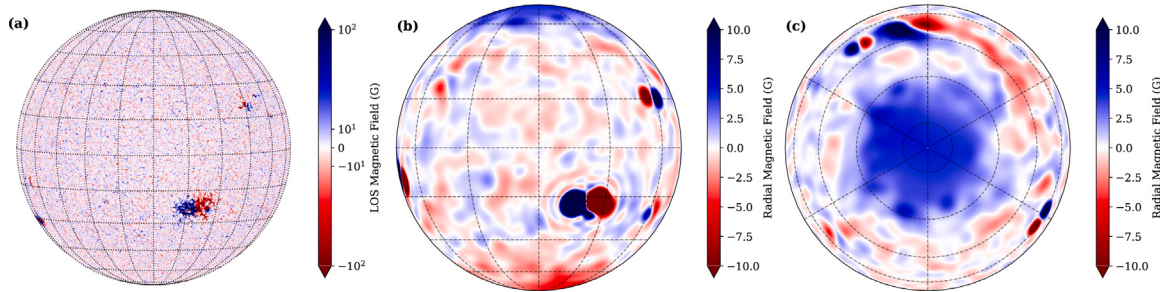


**Fig. 3.** Surface map of the radial magnetic field. (a) HMI full-disk magnetogram on 10.11.2020. (b) SFT model generated a full-disk magnetogram on the same day (considering Gaussian symmetric bipolar magnetic regions). (c) Northern polar view of the same SFT surface map in panel (b).

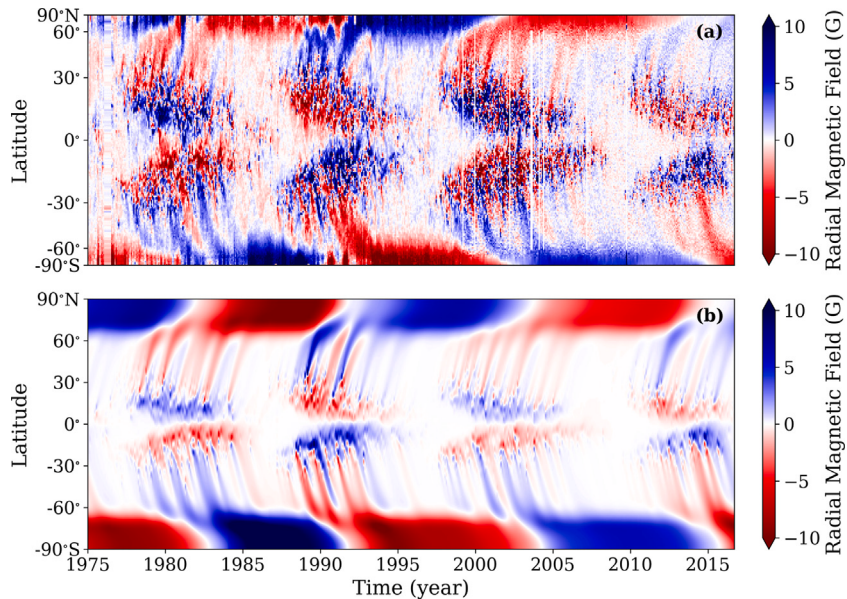


**Fig. 4.** The solar magnetic butterfly diagram. (a) Latitude–time plot of longitudinally averaged radial magnetic field on the solar surface, red and blue denote negative and positive magnetic polarity respectively. The data for Carrington Rotation (CR) 1625–1910, 1911–2096, 2097–2259 is acquired from Kitt Peak Vacuum Telescope (KPVT), Michelson Doppler Imager (MDI) and Helioseismic and Magnetic Imager (HMI) respectively. CR1625 corresponds to a starting date of 1975-02-19. (b) Simulated butterfly diagram using data-driven SFT model (adapted from Bhowmik and Nandy (2018)) for the same time span portrayed in (a). The bipolar magnetic regions are assumed to be symmetrical Gaussian and their statistical properties are extracted from RGO/NOAA database.

Source: Adapted from Nandy et al. (2023).

to the irregular and stochastic nature of the magnetic cycle; for a recent review, see Bhowmik et al. (2023).

The significantly lower amplitude of solar cycle 24 compared to previous cycles elicits interest in understanding the physical mechanisms driving these inter-cycle variations. The primary factors that are involved in modulating the solar cycle amplitude can primarily be listed as (1) random fluctuations associated with transport profiles involved in BL mechanism (Charbonneau and Dikpati, 2008; Nandy et al., 2011; Passos et al., 2014) and (2) the spatiotemporal distribution of anomalous regions and rogue regions (which are deviations from the usual sunspots, violating Joy's tilt law and Hale's polarity rule) on the solar surface (Nandy, 2006; Nagy et al., 2017; Pal et al., 2023).

Studying BL-type solar dynamo model allows having a physical insight into the long-term irregularities and the various magnetic features associated with the solar activity cycle. In this context, past studies show that in a highly diffusive kinematic dynamo model, if the meridional circulation becomes weak during a cycle, that would result in a longer ascending phase of the following cycle (Hathaway et al., 2003; Yeates et al., 2008). Meanwhile, the diffusion becomes dominant to disperse and reduce the toroidal fields, which tends to weaken the

cycle, giving rise to the Waldmeier effect (Hathaway et al., 2003; Karak and Choudhuri, 2011). Besides, the variation of meridional circulation from one cycle to the next cycle and the fluctuations associated with these flows can significantly regulate the variation in magnetic flux at the solar surface and the poles (Nandy et al., 2011; Jiang et al., 2014), which eventually modulate – with finite time delays – the variation in heliospheric open flux and galactic cosmic ray intensity (Wang et al., 2022).

On the other hand, the appearance of multiple anomalous regions (different combinations of anti-Hale and anti-Joy regions) and a single rogue region (anomalous regions with high flux content and high tilt angle) in different phases and activity belts can substantially impact the polar flux build-up that further suppress the strength of the upcoming solar cycle (Nagy et al., 2017; Pal et al., 2023). Results show that the effects on the cycle evolution become noteworthy if the anomalous regions appear near the low latitudinal belts during the middle phase or declining phase of the cycle (Yeates et al., 2015; Nagy et al., 2017; Pal et al., 2023).

Beyond the regular solar activity phases, the extreme effects of solar cycle fluctuations – where the normal cyclic activity ceases to exist,

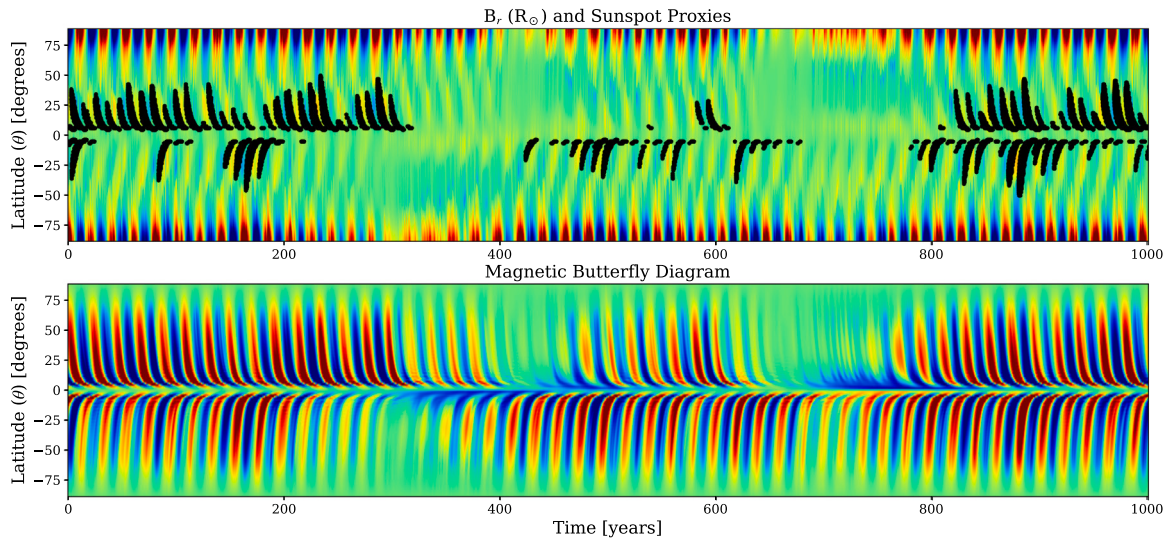


**Fig. 5.** Millennium time-scale simulation of the solar dynamo activity depicting regular cycles and grand solar minima-like episodes. Top panel: evolution of surface radial magnetic field (saturated to 1500G) with the sunspot eruption proxies primarily confined to lower latitudes. Bottom panel: evolution of toroidal magnetic field (saturated to 150kG) at the base of the convection zone.

Source: Adapted from Saha et al. (2022).

and the Sun enters grand minimum episodes along with the changes in the global parity of dynamo solutions can also be addressed with the stochastically forced kinematic solar dynamo model (Usoskin et al., 2005; Passos et al., 2014; Hazra et al., 2014; Hazra and Nandy, 2019). In this context, Fig. 5 illustrates simulated solar grand minima episodes by introducing random fluctuations in the poloidal source terms of the BL-type kinematic solar dynamo model. It is interesting to note the persistence of weak magnetic activity in the solar interior and the poles during such apparently quiescent phases of grand solar minima sustained by mean-field  $\alpha$ -effect in conjunction with the meridional plasma flow (Saha et al., 2022).

The correlation between the averaged polar flux or the dipole moment at the end of the cycle and the next cycle amplitude (see Fig. 6) suggests that polar field proxies impose critical constraints on the solar dynamo process (Yeates et al., 2008; Muñoz-Jaramillo et al., 2012; Karak and Nandy, 2012; Hazra et al., 2020a) and the window for reliable prediction is nearly about half-a-solar cycle (Karak and Nandy, 2012). Thus, reproducing the past polar flux evolution utilizing the data-driven SFT model aids in understanding the polar field build-up and its magnetic polarity reversal (Upton and Hathaway, 2013; Bhowmik and Nandy, 2018; Bhowmik, 2019). Such a model also opens up the possibility of predicting the polar field at different stages of the solar cycle using artificial sunspot data profiles constructed based on observation (Jiang et al., 2013). While assimilating the observed statistics of the emergence of ideal bipolar sunspot pairs during the last 100 years in their calibrated century-scale, data-driven SFT coupled 2D kinematic solar dynamo model, Bhowmik and Nandy (2018) achieve a good match with the past observed polar field evolution and the last eight solar cycles amplitudes. Bhowmik and Nandy (2018) also demonstrate that predicting the polar field at the solar minimum is possible during the declining phase of the ongoing solar cycle, thereby allowing extension of the prediction window for the following cycle beyond half-a-solar cycle. Their prediction suggests a weak-moderate amplitude for solar cycle 25 (see Fig. 7). Apart from these obvious advantages, the progress of model-based forecasting has further strengthened our understanding of the physical processes involved in the solar cycle evolution (Upton and Hathaway, 2013; Bhowmik and Nandy, 2018; Nandy, 2021). The consensus among the physical model-based forecasts of solar cycle 25 has strengthened its acceptability in the community (Nandy, 2021).

The detailed study of observed north–south hemispheric asymmetry present in the sunspot numbers and the polar flux (see Fig. 2) sheds light on the signature of the stochasticity associated with the physical processes in the convection zone. Bhowmik (2019) establishes that the hemispheric asymmetry present in the poloidal field source at cycle minimum originating from the BL mechanism is capable of inducing significant asymmetry in hemispheric sunspot activity in the following solar cycle. To summarize, reproducing and predicting the cycle amplitude, starting epoch, peak amplitude epoch and duration of a cycle requires an accurate accounting of observed active regions emerging in the previous cycle as well as knowledge of the plasma flows may also influence variations in solar activity (Lekshmi et al., 2019).

It is expected that an improved understanding of the interplay between randomness in sunspot pair emergence (anomalous active regions) and fluctuations in flux transport processes will lead to more accurate solar cycle predictions (Bhowmik et al., 2023; Pal et al., 2023).

## 2.5. Solar forcing on the interplanetary medium

Solar forcing is the primary driver for the climate and atmospheric evolution of the Earth and Earth-like planets. The evolving surface magnetic field determines the coronal magnetic field distribution (see Fig. 8), which further modulates the heliosphere's electromagnetic and particulate state through the cumulative effects of the coronal eruptive events, the Sun's open magnetic flux, solar wind, cosmic ray modulation potential, solar wind, and total solar irradiance variations (Cane et al., 1999; Fisk, 1980; Fisk and Schwadron, 2001; Mackay and Yeates, 2012; Potgieter, 2013; Hazra et al., 2015; Cranmer and Winebarger, 2019; Vidotto, 2021). Essentially it is the open coronal field lines that traject solar magnetic flux out to the heliosphere. These open field lines can originate from coronal holes confined usually at higher latitudes (Wang et al., 1996) and also from low- and mid-latitude active regions during coronal mass ejections and other eruptive events (Luhmann et al., 1998; Schrijver and DeRosa, 2003; Owens and Crooker, 2006), wherein, the latter one is found to have a more significant contribution toward heliospheric magnetic flux injection (Wang et al., 2022). Since the coronal field shapes the solar wind, controls the dynamics of eruptive events, plays an important role in coronal heating, and generates a wide variety of different phenomena (Cranmer and

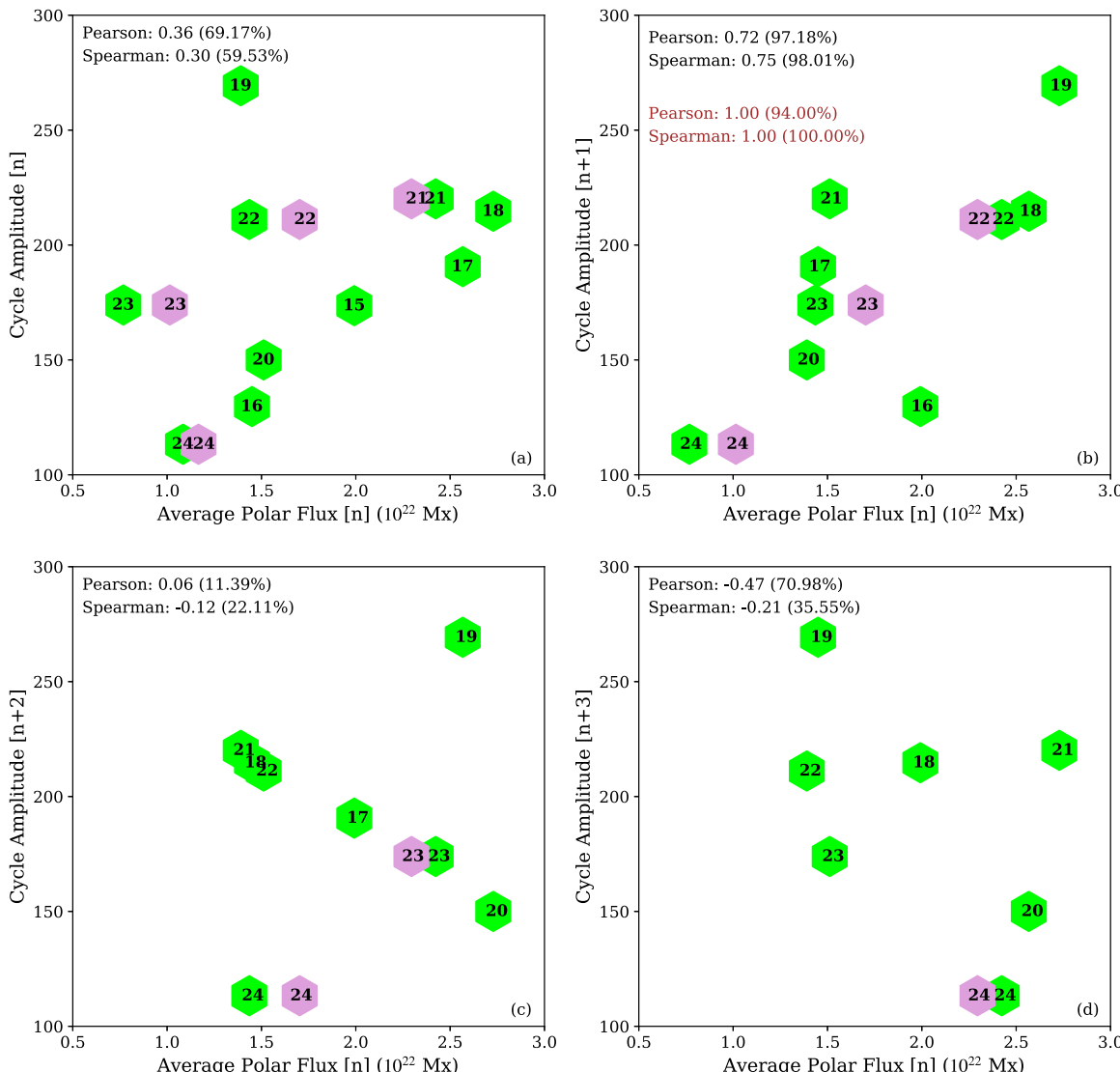


**Fig. 6.** Observed correlation plots between polar flux at solar minimum and solar cycle amplitude . Panel (a), (b), (c) and (d) represent the correlation between the average polar flux for  $n$ th solar cycle minima and the solar cycle amplitude for cycle  $n$ ,  $n+1$ ,  $n+2$  and  $n+3$ , respectively. Green-filled and magnet-filled hexagons denote the average polar flux data and average dipole moment respectively. Both of them are calibrated accordingly to place in the same plot. Wilcox Solar Observatory (WSO) data have been used for average dipole moment calculations and polar faculae data have been utilized for average polar flux calculations. Pearson and Spearman correlation coefficients are mentioned in each plot (black for polar faculae data and red for dipole moment data).

Source: Adapted from [Nandy \(2021\)](#).

[Winebarger, 2019](#)), it is crucial to know the coronal field and its evolution. However, measuring the magnetic fields in the solar corona is difficult due to the low plasma density in the corona and the bright surface radiation in the background, requiring extremely sensitive polarization measurements, thereby necessitating coronal magnetic field modeling.

During a total solar eclipse, the radiation from the solar surface is occulted, which aids in observing the multiple radii long streamers and the million-degree hot solar corona. Thus to know the nature of the coronal magnetic field, eclipse observations are mostly utilized ([Nandy et al., 2018](#); [Dash et al., 2019, 2020a](#)). Eclipse observation, as well as observed coronal images obtained by occulting the center disk, help in validating the model-generated coronal magnetic field. For example, using various numerical and theoretical models, [Mikić et al. \(2018\)](#), [Nandy et al. \(2018\)](#), [Pasachoff et al. \(2018\)](#) predict the coronal structure during the total solar eclipse that occurred on 21 August 2017 across the United States, which captured intricate structures in the coronal magnetic field, including streamers, polar plumes, and prominences.

Modeling prominences (also known as solar coronal filaments), which are observed in the lower part of the corona, using numerical simulations ([Bhowmik and Yeates, 2021](#); [Bhowmik et al., 2022](#)) are crucial to predict eruptive phenomena like CMEs. Moreover, the spatiotemporal distribution of prominences observed over multiple solar cycles demonstrates their capability to signal the epoch of the polarity reversal of the Sun's polar field ([Mazumder et al., 2018](#); [Mazumder, 2019](#); [Mazumder et al., 2021](#))

Beyond studying the localized and short-lived eruptive coronal structures, understanding the global coronal magnetic field evolving over many solar cycles is equally important as the solar wind continuously drags this field out into the solar system, forming the heliospheric magnetic field (HMF) as well as the interplanetary magnetic field (IMF), that spreads through the entire heliosphere ([Owens and Forsyth, 2013](#)). At the solar minimum, HMF is well approximated by a dipolar-like magnetic field structure with the fast solar wind pervading the high-latitude heliosphere and the helmet streamers confined to the near-equatorial region. Also, during this lower activity period, CMEs are much less frequent and are mainly observed near low latitudes ([St. Cyr et al.,](#)

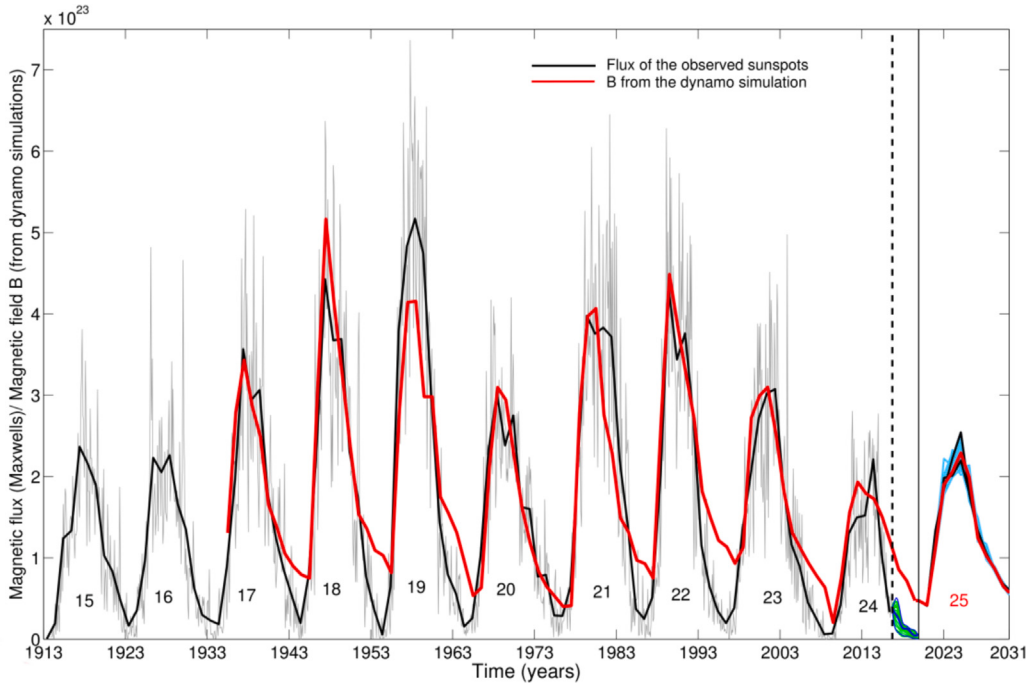


**Fig. 7.** Solar cycle simulation and prediction using data-driven SFT coupled solar dynamo model. Black curves denote the observed magnetic cycle (unsigned calibrated magnetic flux). Background gray curves depict the monthly averaged magnetic flux and magenta curves represent the simulated time series for solar cycle 17 to cycle 25. Predicted solar cycle 25 seems to be similar or slightly stronger than the old solar cycle 24 (see Bhowmik and Nandy, 2018).

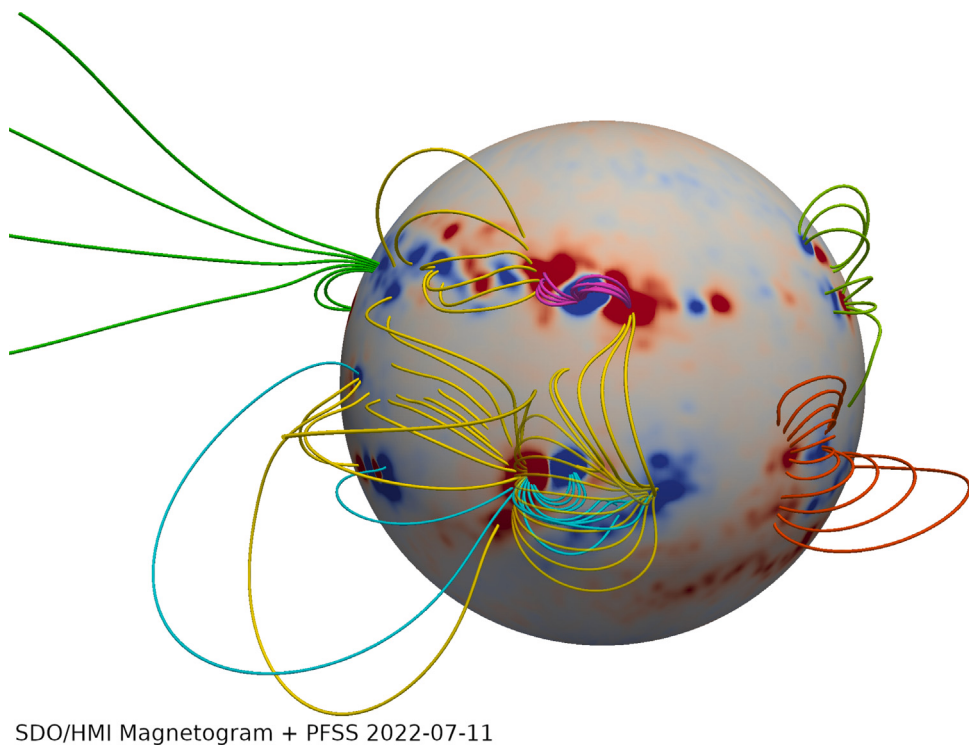


**Fig. 8.** Large-scale magnetic field configuration of the solar corona. Potential field extrapolation on the HMI recorded magnetogram with a Gaussian smoothing filter. Different colored field lines are for representation only. The bright streamer-like regions in the coronagraph observations are aligned with the large-scale fields.

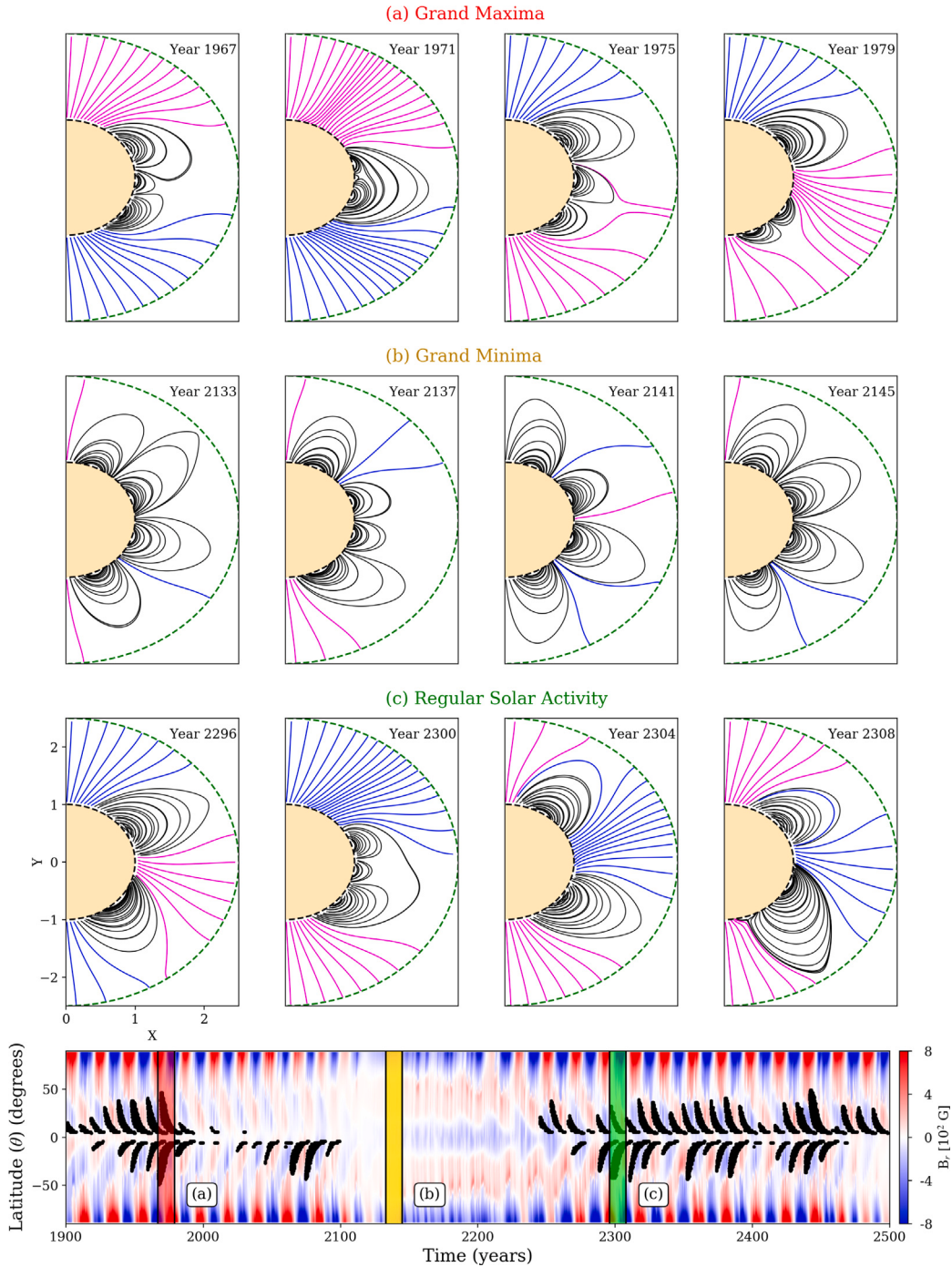


**Fig. 9.** Evolution of the large-scale solar coronal structure during regular and extreme phases of the solar dynamo activity.  
Source: Adapted from Dash et al. (2022).

2000). As the solar cycle progresses, the sunspot number increases and the coronal magnetic field morphology becomes more complex, consequently, CMEs become more frequent along with increasing total open solar flux, which further impacts the near-Earth environment.

It is intriguing to understand the complex structures of the coronal magnetic field during diverse epochs – grand minimum, grand maximum and regular activity phases (Hayakawa et al., 2020; Dash et al., 2022). The impact of variable solar forcing via coronal magnetic fields on the state of the heliosphere during such large fluctuations explains modulations in cosmogenic isotope-based solar activity reconstructions (Dash et al., 2022). Fig. 9 represents one such evolution of

solar coronal magnetic field configuration during the grand maxima, grand minima and regular solar activity phase.

### 3. Impact of solar variability on planetary environments magnetosphere

The activity of the Sun manifests through radiative, particulate, magnetic and solar wind variability, which regulate planetary space environments – including magnetosphere-ionosphere systems such as that of the Earth – giving rise to space weather. Hazardous space weather conditions can have extensive economic and societal consequences as

they can disrupt telecommunications, navigation, satellite operations, orbital lifetime, and can also damage electrical power grids. With an ever-increasing dependence on technology, space weather impacts have become more relevant to human society; thus, it has garnered significant interest not only in the scientific community but also among the general population. This makes the understanding, and forecasting of solar events that regulate space weather, imperative.

### 3.1. Coronal magnetism and the drivers of space weather

The Sun's outer atmosphere – the corona – is a bridge between the activity of the Sun and its impact on the heliosphere and solar system planets. The emergence and evolution of magnetic fields through the solar photosphere creates a changing lower boundary which governs the state of the chromosphere and the corona. Sometimes, rapid restructuring of magnetic fields in the corona create solar storms which lead to severe space weather.

The origin of severe space weather events can be traced back to the sudden release of electromagnetic and kinetic energy which is stored in complex magnetic structures in the solar corona. While the large-scale global coronal field can be assumed to be in the current-free, lowest energy state (i.e., potential field configuration) during quiet conditions, the active corona could be a very dynamic environment in the presence of active regions of large-scale magnetic structures such as filaments. In the latter scenario, often excess non-potential energy becomes concentrated locally in magnetic field lines forming twisted flux ropes or sheared arcades (Mackay and Yeates, 2012).

The growth of nonpotentiality in the coronal magnetic field occurs through two processes. Firstly, the rapid (often immediate) increase happens due to the emergence of highly-twisted sunspots on the surface (Yeates and Bhowmik, 2022), and secondly, a slow build-up occurs due to the differential rotation of the plasma on the solar surface, which acts as a steady source for injection of nonpotential energy in the corona (Bhowmik and Yeates, 2021; Bhowmik et al., 2022). Under certain circumstances, because of magnetic reconnection and plasma instability, these coronal structures – containing excess energy in the forms of current and magnetic helicity – can become unstable and trigger transient eruptions such as solar flares and coronal mass ejections, which are often associated with solar energetic particle events (Shibata and Magara, 2011; Chen, 2011; Desai and Giacalone, 2016; Toriumi and Wang, 2019). The primary agents of adverse space weather are:

- **Solar flares** are intense outbursts of electromagnetic radiation that can disrupt high-frequency radio communication and can also heat up the atmosphere leading to satellite orbital decay.
- **Coronal mass ejections (CMEs)** are enormous expulsions of plasma embedded in magnetic fields which when Earth-directed generate geomagnetic storms, which will be discussed later in this section.
- **Solar energetic particle (SEP) events** are characterized by a sudden increase in particle fluxes observed when particles are accelerated to very high energies by a solar flare or a CME reach Earth. They are known to cause damage to electronic equipment onboard satellites and pose a threat to astronauts.
- **High-speed streams (HSS)** emerging from coronal holes on the Sun interact with the relatively slower ambient solar wind to form stream interaction regions (SIRs) which are regions of compressed plasma and magnetic fields. These events on arrival at Earth can considerably impact the Earth's magnetosphere.

These transient solar phenomena take a finite but short time, on the order of a few hours to a few days, to influence the near-Earth environment, which is why continuous near Sun observation is essential for forecasting their impact on terrestrial atmospheres. A number of satellites including the Solar Dynamics Observatory (SDO), Solar and Heliospheric Observatory (SOHO), Hinode, Solar Terrestrial Relations Observatory (STEREO), BepiColombo, Geostationary Operational

Environmental Satellite (GOES), Reuben Ramaty High Energy Solar Spectroscopic Imager (RHESSI), Wind, Advanced Composition Explorer (ACE), Deep Space Climate Observatory (DSCOVR) and the new age Solar Orbiter (SolO) and Parker Solar Probe (PSP), have been deployed to continuously monitor the solar corona across different wavelengths and from multiple vantage points, and to study the in situ solar wind magnetic and plasma properties (Schwenn, 2006).

Solar flares are among the most explosive events in the solar system. They emit radiation in the entire electromagnetic spectrum but are more significantly observed in X-rays. Based on the peak flux in the soft X-ray range (1–8 Å) as detected by the GOES satellites, solar flares are classified as A, B, C, M, or X, with an A ( $< 10^{-7}$  W/m<sup>2</sup>) class flare being a low-intensity flare and X ( $> 10^{-4}$  W/m<sup>2</sup>) class flare being an intense flare capable of causing major radio blackouts on Earth (Fletcher et al., 2011). Very often, solar flares are associated with the eruption of coronal mass ejections (CMEs), although this is not always the case. A typical flare along with an associated halo CME, is shown in Fig. 10. A large number of CMEs are also observed to be associated with eruptive filaments. Multiple studies, for example, Gopalswamy (2011) have established that the speeds of flare-associated CMEs are positively correlated to the peak intensity of the flare. The speed of filament eruption-induced CMEs, especially quiescent filaments, on the other hand, are correlated to the decaying area of the filament as it takes off (Sinha et al., 2019). In general, CMEs caused due to filament eruptions tend to be slower than those caused by solar flares (Sterling and Moore, 2005).

CMEs are considered to be key drivers of space weather. A classic CME, visible in white light coronagraphs, is recognized as a three-part transient structure, typically consisting of a bright core of prominence material, a dark cavity which is believed to contain the magnetic flux rope with cooler embedded plasma, and a relatively faint leading edge (Lepri and Zurbuchen, 2010). Their angular widths vary across a broad range, which mostly arise due to projection effects. CMEs having angular widths  $> 180^\circ$  ( $> 120^\circ$ ) are called halo (partial halo) CMEs. These kind of CMEs, when they erupt from the frontside of the Sun, and are observed by a satellite on the Sun–Earth line, are of special interest to us because they are entirely Earth-directed and a large part of the contained flux rope is expected to impact the Earth's magnetosphere.

A CME having a sustained southward pointing  $z$ -component of magnetic field (measured in geocentric solar ecliptic (GSE) coordinate system) with high magnitude and speed, erupting from within  $\sim 45^\circ$  of the disk center, can magnetically reconnect with the magnetosphere on arrival at Earth and give rise to moderate to severe geomagnetic storms (Wang et al., 2011, 2003; Shen et al., 2017; Zhang et al., 2021; Wang et al., 2002). Geomagnetic storms are characterized by a significant reduction in the magnitude of the horizontal component of Earth's low-latitude magnetic fields (Lakhina and Tsurutani, 2016). HSSs are also capable of generating weak to moderate geomagnetic storms which last for a longer duration of time, typically on the order of a few days, as compared to storms caused by CMEs (Chen et al., 2014). The severity or intensity of a storm is indicated by geomagnetic indices like the Disturbance Storm Time (Dst), SYM-H and Kp indices.

The geoeffectiveness, or the ability of a CME to trigger a geomagnetic storm, is influenced by properties of their solar source regions. CMEs possessing high kinetic energies originate from active regions which are reservoirs of large free energy (Gopalswamy, 2011). The free energies of active regions are reflected in the magnetic helicity (a measure of the twist, writhe and linking of magnetic flux tubes in a closed volume) of the overlying flux ropes, which may erupt to form CMEs (Dasso et al., 2006). A sound understanding of the magnetic helicity of CMEs can facilitate the prediction of the magnetic properties of their near Earth counterparts. Studies such as Pal et al. (2017), Pal (2022) show that the helicity of flux ropes near Sun and after their interplanetary transit remain roughly the same. Furthermore, Sung et al. (2009) have revealed that the helicity flux of CMEs and their kinetic energies are strongly correlated. It has also been established

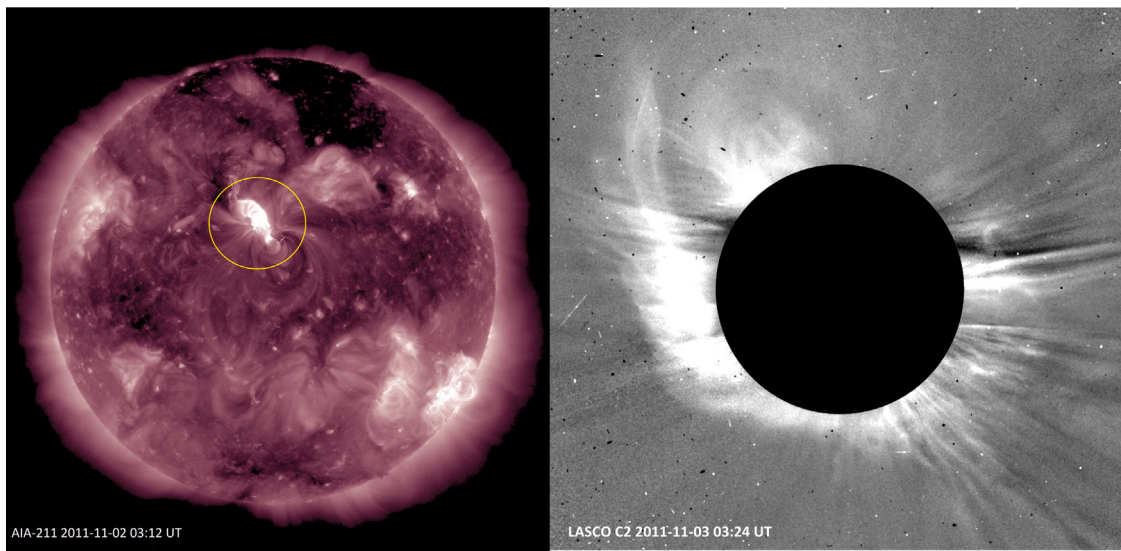


**Fig. 10.** The left panel shows an M1.6 class flare captured in AIA 211 Å channel where the yellow circle encompasses the flaring region. The right panel depicts the associated halo CME in LASCO C2 coronagraph images. These events were observed in 2 November 2011 and caused geomagnetic disturbances at Earth – often termed as “Diwali storm”.

by Pal et al. (2018) that there is a high correlation of CME speeds with the magnetic reconnection flux at their solar source regions.

Geoeffectiveness of an interplanetary structure is also regulated by the medium through which it propagates. As a CME traverses through the interplanetary space, it interacts with the ambient interplanetary magnetic field (IMF). If at any point in space it has a magnetic field orientation opposite to that of the IMF, magnetic reconnection is facilitated. This results in peeling off the twisted outer layer of CME flux ropes (Pal et al., 2021a) and ‘erosion’ of its magnetic flux generally along the azimuthal front which can potentially influence the CME’s ability to affect the Earth’s magnetosphere, or its ‘geoeffectiveness’ (Ruffenach et al., 2015). A schematic diagram of flux erosion of an ICME has been depicted in Fig. 11. CME interactions with other heliospheric large-scale structures including HSS, heliospheric current sheet (HCS), other CMEs encountered in their interplanetary travel, and also, successive CME eruptions (also called quasi-homologous eruptions), can also lead to substantial changes in their shape, orientation, speed and the magnetic content and topology of the flux rope (Shen et al., 2012, 2018; Temmer et al., 2014; Scolini et al., 2020; Lugaz et al., 2017; Heinemann et al., 2019; Pal et al., 2022a; Wang et al., 2018; Moon et al., 2003; Wang et al., 2013; Liu et al., 2017), all of which collectively are capable of diminishing or enhancing its geoeffectiveness.

A problematic scenario arises when an interplanetary counterpart of CME (ICME) that generates a geomagnetic storm on Earth cannot be directly associated with a CME near the Sun or a solar source. These are known as stealth CMEs (Robbrecht et al., 2009; Howard and Harrison, 2013). Stealth CMEs are tricky to deal with since in the absence of the observation of an associated CME, their arrival at Earth cannot be forecast. Even if they can be traced back to a CME, elusive solar source signatures make it difficult to determine if the eruption occurred on the frontside or far side of the Sun. Recently some efforts have been made toward understanding the origin, behavior of such events, as described in Nitta et al. (2021), Palmerio et al. (2021) and predicting their magnetic fields (Palmerio et al., 2021). However, these stealth events remain a challenge toward establishing causal connections between solar driven geospace perturbations.

### 3.2. In situ observations of solar eruptive events

A CME takes about 1–5 days to reach Earth. The arrival of an ICME near Earth is marked by distinct changes in the magnetic field and

plasma properties which distinguish them from the ambient solar wind. A typical ICME drives a shock in front of it, which is observed as a sharp increase in magnetic field intensity, proton speed, density and temperature, succeeded by a turbulent sheath region (Kilpua et al., 2017), which also plays a role of enhancing the ICME geoeffectiveness (Xu et al., 2019). This is followed by the flux rope of the ICME. It is identified as a structure having high magnetic field intensity, low density, low temperature and a low plasma beta. A flux rope is identified as a magnetic cloud (MC) if it has a high magnetic field strength, a smooth rotation in the magnetic field components and low temperatures (Burlaga et al., 1981). Fig. 12 describes an in situ observation and a schematic of a structured solar wind obtained from PSP instruments at the inner heliosphere ( $\sim 0.5$  au).

Stream interaction regions (SIRs) and corotating interaction regions (CIRs) which form due to the interaction of high-speed solar wind streams with the ambient solar wind, on the other hand, are interplanetary structures that do not generally form shock fronts and generate geomagnetic storms with longer recovery duration as compared to CME driven storms, i.e. of the order of a few days. They are characterized by a gradual increase in solar wind speed and a maximum total pressure when the stream interface arrives at the spacecraft (Jian et al., 2006). Compressed magnetic fields, increase in proton density and high temperatures are also observed when the stream interface crosses the spacecraft (Chi et al., 2018).

A moderately fast CME takes about 40 min to reach Earth from Lagrange point L1 where most of the spacecraft taking the in-situ measurements are positioned. This provides a very small window to minimize potential damage from the perspective of forecasting such events. Hence, it is the need of the hour to be able to predict the Earth-arrival times of CMEs and also their properties that may determine their magnetospheric impact by studying their near Sun signatures. In the case of solar flares, since they are electromagnetic radiation propagating through the heliosphere, they take just a few minutes to reach Earth. Therefore, it is important to study the source active regions of solar flares to be able to predict their occurrence with appreciable time in hand.

### 3.3. Predictability of space weather events

The major challenge in predicting space weather is the dynamic nature of solar activities which require information from high dimensional data. The chance of occurrence of a flare depends on the magnetic

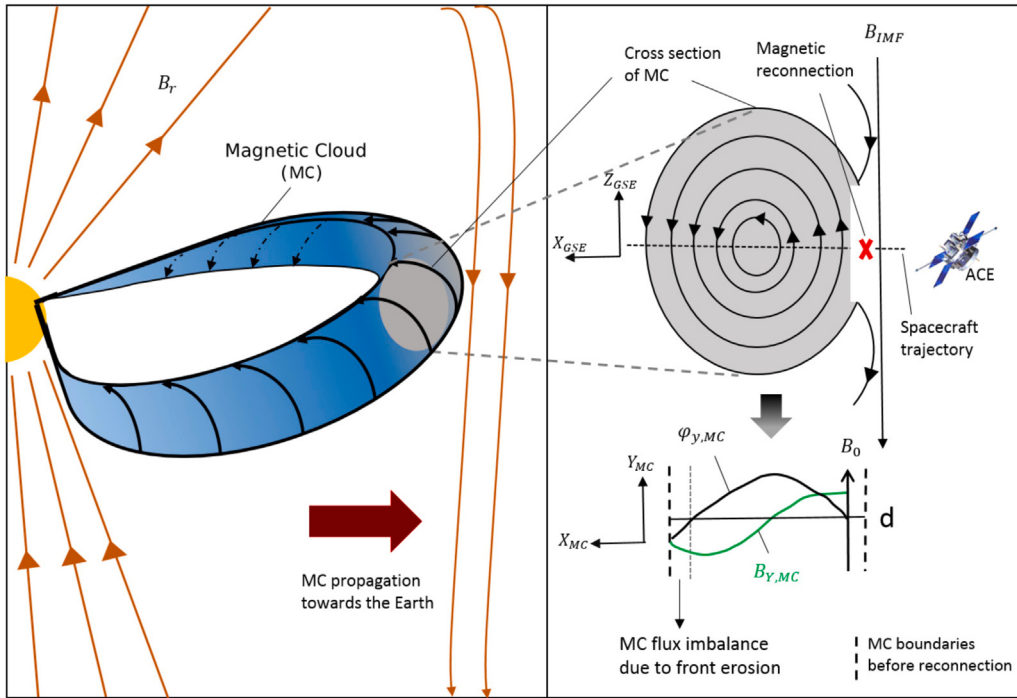


**Fig. 11.** A schematic diagram of flux being eroded from an erupting Earthward CME due to magnetic reconnection with the IMF draping it. Source: Adapted from Pal et al. (2020).

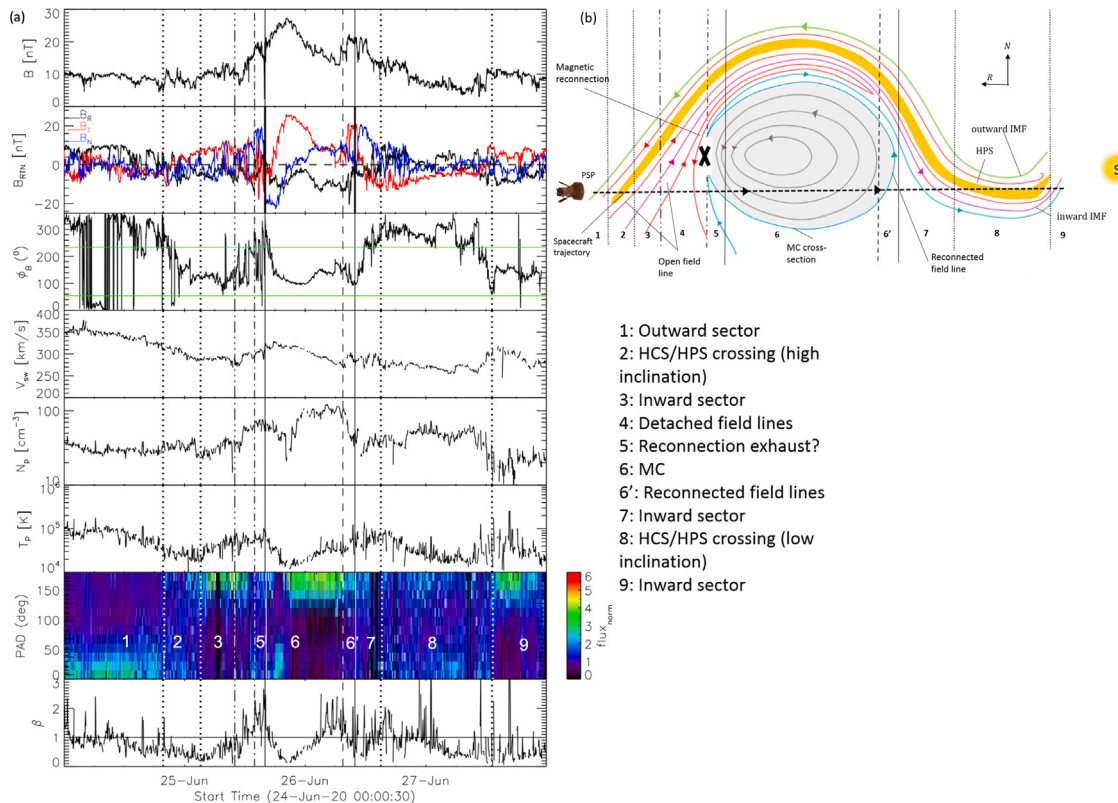


**Fig. 12.** (a) In situ observation of solar wind magnetic parameters (intensity  $B$ , vector field  $B_{RTN}$ , magnetic field longitude angle  $\phi_B$ ), plasma parameters (velocity,  $V_{sw}$ , density  $N_p$ , temperature  $T_p$ , and proton beta  $\beta$ ), and suprathermal electron's pitch angle distribution (PAD) at 283.9–352.9 eV range obtained from PSP instruments at a heliocentric distance  $\sim 0.5$  au. The observation shows HCS and IMF draping about a flux rope associated with a streamer blowout CME. (b) A schematic obtained by following the PSP in situ observation. The annotated regions indicate the different structures in the observed solar wind. Source: Adapted from Pal et al. (2022a).

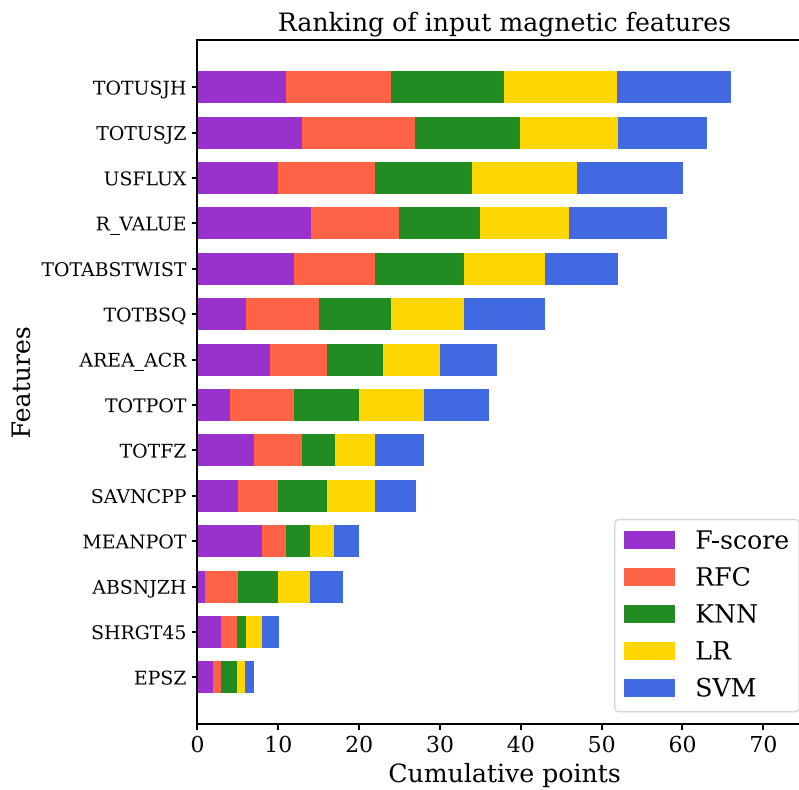


**Fig. 13.** The figure demonstrates the combined ranking of input magnetic features as described in [Sinha et al. \(2022\)](#). Input magnetic features are shown in Y axis and the cumulative points for each magnetic features are shown in the X axis.

properties of the active region. Complex active regions with non-potential magnetic fields often produce intense flares via the process of magnetic reconnection.

Numerous attempts have been made to predict the occurrence of solar flares. Initial attempts, like those of [Leka and Barnes \(2003\)](#), [Barnes et al. \(2007\)](#) were based on statistical approaches using multiple parameters to distinguish between flaring and non-flaring active regions. Physics based methods such as the one proposed by [Kusano et al. \(2020\)](#) have propelled the field forward by accurately identifying active regions which have the potential to flare and predict intensity of the flare, and have highlighted the importance of twist flux density for understanding flare onset mechanisms. Recent advancement in machine learning aids in space weather forecasting by using active region magnetic fields properties obtained from the magnetograms of the Solar and Heliospheric Observatory (SOHO) Michelson Doppler Imager (MDI) and the Solar Dynamics Observatory (SDO) Helioseismic and Magnetic Imager (HMI), as discussed in [Yu et al. \(2009\)](#), [Song et al. \(2009\)](#), [Yuan et al. \(2010\)](#), [Huang et al. \(2018\)](#), [Bobra et al. \(2014\)](#), [Dhuri et al. \(2019\)](#), [Hazra et al. \(2020b\)](#) among others.

In a comparative analysis with multiple supervised machine-learning algorithms, [Sinha et al. \(2022\)](#), [Iwai et al. \(2021\)](#) have demonstrated that Logistic Regression and Support Vector Machine perform particularly well in identifying the flare-prone active regions and highlighted key magnetic features like current helicity, unsigned flux, flux near the polarity inversion line, current density and magnetic twist are among the most influential in determining flaring capability of active regions. Apart from support vector machine and logistic regression, k nearest neighbor, random forest classifier and anova F-test methods have been used for producing this combined ranking of input magnetic features. [Fig. 13](#) demonstrates the global ranking of input magnetic features based on their usefulness in the classification task (For details see [Sinha et al., 2022](#)).

As previously discussed, CMEs also play a crucial role in shaping the near-Earth space environment. CMEs' near-Sun 3-D speeds and

morphology can be studied by forward modeling them with the Graduated Cylindrical Shell (GCS) model ([Thernisien et al., 2006](#)). These parameters can be fed as input to the drag-based models, for example, [Dumbović et al. \(2018\)](#), to quickly predict the arrival time of CMEs near 1 AU. However, the prediction of their geoeffectiveness is a more challenging task because of various distortions in morphology, changes in orientation and propagation direction that CMEs endure during their transit through the interplanetary space. Attempts have been made to predict the magnetic properties of CMEs near 1 AU using data-driven magnetohydrodynamical modeling ([Manchester et al., 2004](#); [Shen et al., 2014](#); [Iwai et al., 2021](#)), but they are computationally expensive and there is not enough near real time data from interplanetary space to serve as input for precise results. Alternatively, several semi-empirical models have been proposed to predict the magnetic structure of flux ropes near 1 AU ([Savani et al., 2015](#); [Kay and Gopalswamy, 2017](#); [Möstl et al., 2018](#); [Sarkar et al., 2020](#); [Pal et al., 2022b](#)). [Pal et al. \(2022b\)](#) have developed a framework that predicts the arrival time, average speeds, and magnetic profile of CMEs near Earth, and also the duration of passage of the CME, based on observations near Sun, assuming the flux rope expands into the heliosphere self similarly. Such modeling approaches establish a forecasting ability for CMEs and can conceivably aid in predicting their magnetospheric impact in the future.

### 3.4. Magnetohydrodynamical understanding of CME forced geo-magnetosphere and estimation of geoeffectiveness

It is known that the magnetic activities of the Sun influence the magnetic structure around the Earth, giving rise to space weather disruptions. However, mankind cannot understand space weather around Earth based on spacecraft observations only. It is hard to understand a three-dimensional structure with single-point measurements and we need more spacecraft observations for adequate data inputs from every corner. Thus, we rely on physics-based modeling of the magnetosphere

to understand the space environment of our planet. In 2019, we developed the Star Planet Interaction Module, CESSI-SPIM (Das et al., 2019) that describes how the solar wind, containing “frozen-in” plasma and solar-originated magnetic fields, (Parker, 1958) accelerating through the interplanetary medium forces the Earth’s quasi-dipolar magnetic field to form a ubiquitous tear-drop shaped magnetosphere with a bow shock ahead of it (Schwartz, 1985; Kallenrode, 2001; Liu and Fujimoto, 2011, and references therein). But eventually, this solar forcing of the magnetosphere considerably intensifies and turns into a geomagnetic storm when the Earth faces an Interplanetary CME or ICME (Webb, 1995; Hudson, 1997; Koskinen and Huttunen, 2007, and references therein). Being the heliospheric ( $> 50R_{\odot}$ ) counterpart of CMEs, ICMEs undergo significant deceleration due to the drag of surrounding solar wind but remain supersonic at 1 AU and hence are escorted by an interplanetary shock (Schwenn and Marsch, 1991b;a; Manoharan et al., 2004; Zurbuchen and Richardson, 2006; Kilpua et al., 2017, and references therein). It also possesses a magnetic cloud, a flux-rope structure of magnetic field stronger than the surrounding solar wind (Burlaga et al., 1982; Gosling, 1990; Farrugia et al., 1997; Owens et al., 2005, and references therein). Consequently, interactions between the magnetosphere and the tremendous energy of an ICME are responsible for space weather disturbances around Earth (Koskinen and Huttunen, 2006; Gopalswamy, 2007).

To quantify the geoeffectiveness (capability of causing a geomagnetic disturbance) of an incoming ICME by measuring the change in the horizontal geomagnetic field ( $H$ ), indices like disturbance storm time index ( $Dst$ , Kyoto  $Dst$ ) and  $SYM-H$  were introduced (Menvielle et al., 2011, chap. 8.6). Both of these geomagnetic indices measure the decrease in the magnitude of the axially symmetric component of  $H$ , parallel to the dipole axis of Earth (Wanliss and Showalter, 2006).  $Dst$  is calculated hourly from four ground-based mid-latitudinal observatories (Sugiura, 1964; Sugiura and Kamei, 1991; Nose et al., 2015), whereas,  $SYM-H$  is calculated per minute from six mid-latitudinal observatories (Iyemori et al., 2009). These southward axially symmetric disturbances in the horizontal geomagnetic field are known to be produced by the currents in the equatorial region of the geomagnetic dipolar field – usually recognized as the ring current – the oldest concept in magnetospheric physics (Ganushkina et al., 2017; Ebihara, 2019; Egeland and Burke, 2012, and references therein). In a broad and simplified way, the ring current can be described as an axially symmetric electric current flowing westward around the Earth with variable density at geocentric distances. The charged particles from the ionosphere, as well as trapped solar wind particles, undergoes gyro-motion, grad- $B$  drift motion, and curvature drift motion within the magnetosphere (Parker, 1957) and lead to ring current within the range from 1 to 400 keV of energy. Even though the name ‘ring current’ infers a symmetry in its shape, there exists a partial ring current structure with field-aligned closure ionospheric loops (Williams, 1983; Daglis, 2001; Le et al., 2004) which is azimuthally asymmetric. Most importantly, during geomagnetic storms, due to the dawn–dusk asymmetry of  $H$  and enhancement in the trapping of charged particles from the night-side plasma sheet to the inner magnetosphere, the partial ring current significantly increases and gets stronger on the night side of the Earth than on the dayside. Since  $Dst/SYM-H$  contains contributions from different magnetospheric currents, including these partial ring currents, various models have been implemented to estimate the storm time magnetospheric current and predict the  $Dst/SYM-H$  (Maltsev, 2004, and references therein). The most commonly used techniques are electrodynamics modeling coupled with MHD, low-dimensional magnetosphere-ionosphere modeling, kinetic modeling, empirical modeling using neural networks, etc. Rastäetter et al. (2013) have given a detailed overview and comparison of metric-based results of such models performed in Geo-space environment modeling (GEM) 2008–2009 challenge to predict  $Dst$ . Usually, such models are computationally expensive. On the other hand, models on empirical or machine learning-based schemes usually exhibit good

prediction skills with low computation costs. Still, they cannot describe the global structure of the storm-time magnetosphere. Kinetic and electrodynamics solver-coupled MHD models that can solve geospace physics but are not explicitly fine-tuned for geoeffectiveness prediction. Also, these approaches are computationally heavy and complicated.

Thus, to bridge the gap between the understanding of storm-time magnetosphere and the estimation of geoeffectiveness, we are developing a Storm Interaction Module (CESSI-STORMI) (Roy and Nandy, 2022). In STORMI, we set up a three-dimensional (3D) compressible magnetohydrodynamic (MHD) model in PLUTO (Mignone et al., 2007), similar to CESSI-SPIM. We use a Gold-Hoyle type magnetic flux rope (Gold and Hoyle, 1960; Hu et al., 2014; Wang et al., 2016) to model the ICME that forces a “far-out” planetary magnetosphere. Our data-driven simulation depicts the storm-influenced changes in the magnetosphere. Studies show that the changes in shape in the distant tail lag that in the near-Earth tail, which also lags the changes in the magnetopause area (Walker et al., 1999; Hultqvist et al., 1999). As a result, the time-varying magnetic field of the flux-rope results in a time-varying orientation of the magnetosphere and introduces torsion in the  $\theta$ -shaped current system of the magnetotail (Nakamura et al., 1997; Christon et al., 1998). Also, the magnetosphere gets compressed in the day-side by the enormous ram pressure of the inflow; the magnetopause pushes back to a lower altitude, and the polar cap boundary increases by a large amount. We also notice that, in STORMI, the magnetic field topology around Earth, influenced by the plasma flow, induces current ( $\vec{V} \times \vec{B} = \mu_0 \vec{J}$ ) within the magnetosphere. As projected on the equatorial plane, these induced currents behave similarly to the ring currents (Roy and Nandy, 2021a,b) due to the topology. We use Biot-Savart’s law for electric current density throughout the volume of a conductor to calculate the magnetic field at different equatorial surface points of the Earth due to these currents. We estimate the Storm Intensity (STORMI) index by taking the mean contribution of reduction of the magnetic field at these points as a proxy to the  $Dst/SYM-H$ . Results from the analysis of two contrasting storms from Solar Cycle 23 show that the STORMI index shows a linear behavior with respect to  $Dst$  and  $SYM-H$  with a Pearson’s linearity coefficient of more than 0.8. This result from CESSI-STORMI is comparable and, in some cases, better than the existing models.

Given that the structure of a propagating CME in the heliosphere is changed by the draping interplanetary medium (Pal et al., 2020) and also observed data inputs are possible only at the L1 point near Earth, there is very little time available to make an actual forecast using STORMI. However, with the machine-learning-based prediction of solar flares (Sinha et al., 2022) and prediction of ICME magnetic clouds based on near sun observations (Pal et al., 2018; Pal et al., 2022b) CESSI-STORMI can be utilized to predict the timing and intensity of geomagnetic storms at a much earlier phase.

#### 4. Understanding the magnetic field dynamics around (exo)planets

Thanks to the Kepler mission, thousands of planets outside our solar system have recently been discovered. Dedicated *Kepler* and *TESS* missions also reveal significant statistical information regarding these transiting (exo)planets’ masses, sizes, and orbital separations. One important property of the (exo)planet is the presence or absence of a global magnetic field. Magnetic fields of the (exo)planet play an essential role in determining the properties and structure of the (exo)planetary atmosphere. It is also well known that planetary magnetic fields are generated by a dynamo mechanism that relies on the convection mechanism inside the planetary interior. This realization indicates the necessity of detecting and measuring the (exo)planetary magnetic field as it is one of the few ways to develop an understanding of the structure and dynamics of (exo)planetary interiors and atmospheres. The planetary magnetic field is also an important factor in determining the longevity of the planetary atmosphere as it protects

the planet from the impact of high-energetic particles coming from the stellar wind. In summary, we need a clear understanding of the (exo)planetary magnetic field dynamics to determine whether a planet is habitable or not.

The structure and shape of the (exo)planetary magnetosphere depend on the balance between the magnetic pressure of (exo)planetary magnetic field and the three components of the stellar wind pressure, namely, the dynamic pressure or momentum flux of the stellar wind ions, the kinetic and thermal pressure of the stellar wind plasma, and the magnetic pressure because of the interplanetary magnetic field. Generally, the structure of the planetary magnetosphere consists of four distinct regions – bow shocks, magnetopause, magnetosheath, and magnetotail. The interplay between the stellar wind and (exo)planetary magnetic field is responsible for forming all these four regions. The bow shock is the outer boundary of the planetary magnetosphere where the stellar wind speed drops abruptly because of its approach toward the planet. Interaction between the stellar wind and the (exo)planetary magnetic field also leads to the formation of magnetopause at the day side of the (exo)planet – a position or area where the dynamical ram pressure of the solar wind is equal to the magnetic pressure of the (exo)planetary magnetic field. The region between the bow shock and the magnetopause is known as magnetosheath. While the day side of the planetary magnetosphere is compressed because of the solar–stellar wind, night side of the planetary magnetosphere (also known as magnetotail) extends far beyond. Night-side of the planetary magnetosphere has a swept-back magnetic field forming two lobes of open magnetic field (northern and southern lobe, respectively) with one foot of the magnetic field line connected to the planet. The plasma sheet, a warm and dense plasma region, separates these two lobe regions.

Reconnection at the magnetopause region is thought to be an effective mechanism for coupling the stellar wind with the planetary magnetic field. However, the coupling mechanism is not still well understood. It is necessary to understand how the stellar wind couples with the planetary magnetic field, how this coupling affects the planetary magnetosphere, and how we can quantify that mechanism. Understanding these interactions can help us learn more about the habitability of solar system planets and exoplanets and thus aid in assessing the potential for life beyond Earth.

#### 4.1. Impact of varying stellar activity on (exo)planetary environments

Various studies have been performed in recent years to understand how the stellar wind affects the planetary magnetosphere and how we can quantify them (Nandy and Martens, 2007; Lammer et al., 2012; See et al., 2014; Vidotto and Cleary, 2020; Harbach et al., 2021; Nandy et al., 2021; Hazra et al., 2022; Gupta et al., 2023). Variations in stellar magnetic activity lead to changes in the amount of radiation emitted by the star (Spina et al., 2020), stellar wind speed (Finley et al., 2018), and the strength of the magnetic field of plasma winds (Vidotto et al., 2015). These interconnected phenomena can distort the planetary dipolar field, resulting in a magnetospheric structure that may differ from what is typically observed in the case of Earth. These interactions can explain variations in the observed transit signatures of (exo)planets (Harbach et al., 2021). Detailed understanding of these interactions will also help us to understand the longevity of the (exo)planetary atmosphere, how well the magnetosphere of an (exo)planet can protect its atmosphere from the effects of the stellar winds (See et al., 2014; Gallet et al., 2016; Basak and Nandy, 2021; Gupta et al., 2023).

Das et al. (2019) models the impact of varying stellar wind speed on Earth-like magnetized (exo)planets using CESSI-SPIM, a module based on three dimensional magnetohydrodynamic simulations. The balance between the thermal, magnetic, and dynamic pressures determines the shape and location of the magnetopause. It is evident from Fig. 14 (left panel) that increasing the stellar wind speed leads to greater wind penetration, resulting in the formation of magnetopause closer

to the planetary surface. The orientation of stellar wind relative to the planetary magnetic field plays a crucial role in the formation of the magnetopause as evident from Fig. 15. Magnetopause standoff distance in the case of a northward interplanetary magnetic field (N-IMF) is slightly farther from the planetary surface compared to a southward interplanetary magnetic field (S-IMF) (Pudovkin et al., 1998; Shue and Chao, 2013; Lu et al., 2013; Basak and Nandy, 2021). This can be attributed to the inward or outward migration of the magnetopause layer due to magnetic reconnection at the substellar point and the clustering and external pressure of parallel magnetic field lines, respectively. Fig. 15(a) shows that the reconnection point lies at the subsolar region for the SIMF case, while Fig. 15(c) depicts that for NIMF cases, reconnections occur near polar regions. Observation confirms the varying magnetic activity of the Sun and other Stars during their different evolutionary phases (Nandy, 2004; Nandy and Martens, 2007; Brun et al., 2014; Vidotto, 2021). The study of the young Sun and other young stars can provide insight into the conditions that may have influenced the habitability of early planets. Studies by Lu et al. (2013), Shue and Chao (2013) describe the variation of subsolar magnetopause and cusp with changing IMF. With increasing IMF strength, the magnetopause shifts closer to the planetary surface, and this effect is larger for the southward IMF than for the northward IMF.

A study by Luhmann et al. (1993) compares the long-term behavior of the interplanetary magnetic field (IMF) at two different distances from the sun: 0.7 astronomical units (AU) and 1 AU. The IMF magnitude affects the structure and shape of planetary bow shocks and magnetopause configurations through its influence on the Mach numbers that describe the properties of the solar–stellar wind. The orientation of the IMF also plays a role in determining how effectively the solar/stellar wind can couple with planets. The variability of the IMF on all time scales provides insight into processes occurring in the solar or stellar wind and how much the wind might deviate from its average properties over a given period of time.

A planet's habitability depends on the existence of liquid water on that planet. The temperature at the planetary surface should be within 100° centigrade for the existence of liquid water. This habitability criterion demands the existence and stability of the planetary magnetosphere as it protects the planetary atmosphere from the harmful effects of the stellar wind. It is also found that IMF variability, in conjunction with higher level of stellar magnetic activity, directly impacts the mass loss of the planetary atmosphere (Schillings et al., 2019). It is thus important to figure out the impact of the IMF on the atmospheric mass loss of (exo)planets for determining the habitability of (exo)planets and predicting the long-term stability of their atmospheres.

#### 4.2. Effects of changes in the intrinsic planetary magnetic field on its surroundings

As we discussed earlier, the presence of the (exo)planetary magnetic field is one of the essential conditions for planetary habitability. Magnetospheres act as shields, deflecting the charged particles away from the planet and protecting it from the effects of space weather. However, some planets like Venus and Mars in our solar system do not have their intrinsic magnetic field. Thus question remains whether the intrinsic planetary magnetic field is necessary for the formation of the planetary magnetosphere.

Few recent studies indicate that an imposed magnetosphere surrounds planets with no intrinsic magnetic field (non-magnetized planets) due to the draping of the solar wind magnetic field around that planet (Futaana et al., 2017; Basak and Nandy, 2021). Fig. 15(b) clearly shows that there are no steady-state reconnections in the non-magnetized planet scenario, and stellar magnetic field lines drape around the non-magnetized planet to form an imposed/induced magnetosphere. Fig. 14, (right panel) indicates the stand-off distance (distance between the magnetopause and the planetary surface) is more when the intrinsic planetary atmosphere becomes stronger.

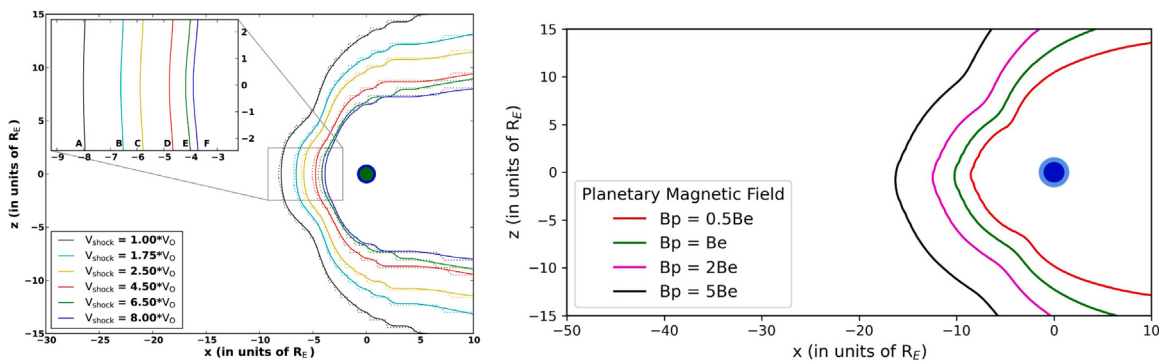


**Fig. 14.** Left: Cases A through F show the magnetopause shape in XZ plane for a range of stellar wind speeds, with case A representing the slowest wind ( $V_0 = 350 \text{ km s}^{-1}$ ) and case F representing the fastest wind at a distance of 1AU. Right: Variation of magnetopause shape in XZ plane with planetary dipolar field strength. Symbol  $R_E$  and  $B_e$  denote, respectively, the radius and magnetic field of Earth.

Source: Adapted from Das et al. (2019).

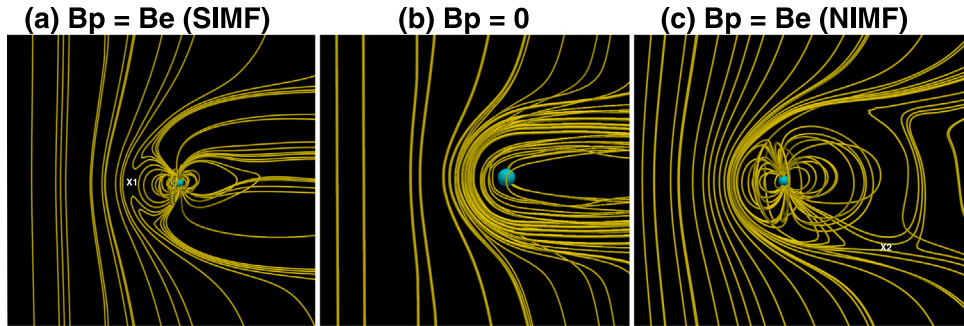


**Fig. 15.** The magnetic field lines depicted in panels (a) through (c) illustrate the impact of the intrinsic magnetic field and the orientation of the IMF on the magnetosphere for planets with and without intrinsic magnetic field. In the southward-pointing IMF case (a), reconnection points (denoted by X1) occur on the dayside of the planet. For the northward-pointing IMF case (c), the reconnections take place near the polar regions, as indicated by X2. When the planet lacks an intrinsic magnetic field (b), there are no steady-state reconnections, and the stellar field lines are found to drape around the planet on the dayside. Here,  $B_e$  denotes the Earth's magnetic field.

Ancient Mars is believed to have had an intrinsic magnetic field similar to the Earth and a thicker atmosphere that allowed liquid water to exist on its surface. Magnetopause is often thought of as a protective shield for a planet. However, previous studies for Mars and Venus have suggested that a planet with a weak intrinsic magnetic field may experience greater atmospheric mass loss than a planet with no intrinsic dipolar field (Sakai et al., 2018; Gunell et al., 2018; Egan et al., 2019). Sakata et al. (2020) investigated the role of an intrinsic magnetic field on the escape of ions from the atmosphere of ancient Mars. They found that the presence of an intrinsic magnetic field can facilitate cusp outflows, which can increase the escape of molecular ions. However, a study by Dong et al. (2018) shows that the rate at which ions escape from the martian atmosphere was much higher compared to present day due to the stronger solar wind and higher ultraviolet fluxes emitted by the young Sun at that time. The role of an intrinsic magnetic field of the planet in protecting atmospheric escape is still a matter of debate.

It is important to understand the near-Earth environment and the impact of the Sun on Earth and other planets. By studying the solar interior and its impact on the near-Earth environment, we can better understand the complex processes that shape our solar and (exo)planetary systems and the conditions necessary for the emergence of life.

## 5. Concluding remarks

To summarize, in this review we have provided an overview of how magnetic fields are created in the Sun's interior, how they vary across timescales ranging from decades to millennia, how their emergence at the surface as sunspots and subsequent evolution driven by plasma flows govern the structuring of the large-scale solar corona,

how magnetic properties of emerged active regions and structures such as filaments drive solar eruptive events, how magnetic flux ropes embedded in solar storms evolve, and eventually how the solar wind and interplanetary magnetic clouds shape and force planetary magnetospheres such as that of the Earth. In some specific cases, we have highlighted how our understanding can lead to assessment of the flaring potential of solar active regions and data-driven predictive models of the geoeffectiveness of solar storms. We have also discussed how understanding gleaned in the context of heliophysics can guide our interpretation of star–planet interactions in (exo)planetary systems that have profound implications for habitability.

As a caveat, we note that we have not covered some aspects of solar variability such as solar spectral irradiance variations and its impact on atmospheric dynamics and climate, neither have we covered solar energetic particles and the origin and driving of solar wind, plumes and jets, e.g. These are important topics that are covered in other extant literature by independent experts.

It would also be naive to pretend we know everything. There are several outstanding challenges that remain. These include but are not limited to, elucidating how the Sun enters phases of extreme solar activity episodes such as grand minima and maxima, the origin of super-modulation (i.e., very long-term variations) in magnetic activity, the exact physical mechanisms that cause solar eruptive events, constraining the evolution of solar wind and interplanetary storms through the heliosphere and developing, early, and accurate space weather forecasting capabilities for all heliospheric forcing parameters of solar origin.

While we have not delved in to instrumentation and space missions relevant for heliophysics, we are in an era where recently launched missions such as Parker Solar Probe and Solar Orbiter are returning

new information that in conjunction with existing missions will help establish further causality across the Sun–Earth domain. China's recent launch of Kuafu-1 and India's upcoming launch of the Aditya-L1 space mission are expected to further add to the suite of heliophysics observatories, including the ability of sustaining long-term observations solar spectral irradiance variability across wavelengths most relevant for the Earth's climate (Tripathi et al., 2017). NASA's PUNCH (Polarimeter to Unify the Corona and Heliosphere) mission will add to our capability of connecting physics occurring in the Sun's atmosphere to the heliospheric manifestations. There are missing elements in our suite of heliophysics observatories. Multi-vantage point mission concepts to characterize the state of the inner heliosphere and interplanetary space, including extreme out-of-ecliptic missions to explore the Sun's polar regions can return transformative new information to constrain the flow of energy, plasma and magnetic fields that bridge the Sun to Earth and other planets (Nandy et al., 2023; Hassler et al., 2023).

In hindsight, if one steps back and assesses the causality across the domain of heliophysics, one is left with an overwhelming sense of awe at the knowledge we have acquired; of how physical mechanisms in the interior of a distant star, our Sun, is intimately connected to the fate of our home planet, the Earth, and how variations in solar output that originate within the Sun's interior influence our technologies and life. This causality is perhaps most beautifully illustrated in the discovery that once surface magnetic fields spawn a magnetic storm, its space weather impact is influenced by flux erosion of the magnetic storm during its interplanetary passage through the ambient heliospheric open flux – which in turn is governed by the slow evolution of magnetic fields driven by the solar dynamo functioning in the Sun's interior (Pal et al., 2020)!

### Declaration of competing interest

The authors declare that they have no known competing financial interests or personal relationships that could have appeared to influence the work reported in this paper.

### Data availability

Data will be made available on request.

### Acknowledgments

CESSI is funded by IISER Kolkata, Ministry of Education, Government of India. S.D. acknowledges the INSPIRE fellowship received from the Department of Science and Technology, Government of India. S.R. & C.S. acknowledge financial support from the Council for Scientific and Industrial Research, Government of India. S.S., S.P. & S.G. acknowledge financial support from the University Grants Commission, Government of India. D.N. acknowledges useful discussions facilitated by Working Groups at the Scientific Committee on Solar-Terrestrial Physics (SCOSTEP), the International Space Weather Action Team of the Committee on Space Research (COSPAR) and Commission E4 (Impact of Magnetic Activity on Solar and Stellar Environments) of the International Astronomical Union (IAU).

### References

- Alfvén, H., 1942. Remarks on the rotation of a magnetized sphere with application to solar rotation. *Arkiv Matematik, Astronomi Och Fysik* 28A, 1–9.
- Babcock, H., 1961. The topology of the sun's magnetic field and the 22-YEAR cycle. *Astrophys. J.* 133, 572.
- Barnes, G., Leka, K., Schumer, E., Della-Rose, D., 2007. Probabilistic forecasting of solar flares from vector magnetogram data. *Space Weather* 5 (9).
- Basak, A., Nandy, D., 2021. Modelling the imposed magnetospheres of Mars-like exoplanets: star-planet interactions and atmospheric losses. *Mon. Not. R. Astron. Soc.* 502 (3), 3569–3581. <http://dx.doi.org/10.1093/mnras/stab225>.
- Basu, S., Antia, H.M., Tripathy, S.C., 1999. Ring diagram analysis of near-surface flows in the sun. *Astrophys. J.* 512 (1), 458–470. <http://dx.doi.org/10.1086/306765>, arXiv:astro-ph/9809309.
- Bhowmik, P., 2019. Polar flux imbalance at the sunspot cycle minimum governs hemispheric asymmetry in the following cycle. *Astron. Astrophys.* 632, A117. <http://dx.doi.org/10.1051/0004-6361/201834425>.
- Bhowmik, P., Jiang, J., Upton, L., Lemerle, A., Nandy, D., 2023. Physical models for solar cycle predictions. <http://dx.doi.org/10.48550/arXiv.2303.12648>, arXiv e-prints arXiv:2303.12648.
- Bhowmik, P., Nandy, D., 2018. Prediction of the strength and timing of sunspot cycle 25 reveal decadal-scale space environmental conditions. *Nature Commun.* 9, 5209. <http://dx.doi.org/10.1038/s41467-018-07690-0>, arXiv:1909.04537.
- Bhowmik, P., Yeates, A.R., 2021. Two classes of eruptive events during solar minimum. *Sol. Phys.* 296 (7), 109. <http://dx.doi.org/10.1007/s11207-021-01845-x>, arXiv: 2107.01941.
- Bhowmik, P., Yeates, A.R., Rice, O.E.K., 2022. Exploring the origin of stealth coronal mass ejections with magnetotriboctional simulations. *Sol. Phys.* 297 (3), 41. <http://dx.doi.org/10.1007/s11207-022-01974-x>.
- Bobra, M.G., Sun, X., Hoeksema, J.T., Turmon, M., Liu, Y., Hayashi, K., Barnes, G., Leka, K.D., 2014. The helioseismic and magnetic imager (HMI) vector magnetic field pipeline: SHARPs - space-weather HMI active region patches. *Sol. Phys.* 289 (9), 3549–3578. <http://dx.doi.org/10.1007/s11207-014-0529-3>, arXiv:1404.1879.
- Braun, D.C., 2019. Flows around averaged Solar Active Regions. *Astrophys. J.* 873 (1), 94. <http://dx.doi.org/10.3847/1538-4357/ab04a3>.
- Brun, A.S., García, R.A., Houdek, G., Nandy, D., Pinsonneault, M., 2014. The solar-stellar connection. *Space Sci. Rev.* 196 (1–4), 303–356. <http://dx.doi.org/10.1007/s11214-014-0117-8>.
- Brun, A.S., Miesch, M.S., Toomre, J., 2004. Global-scale turbulent convection and magnetic dynamo action in the solar envelope. *Astrophys. J.* 614 (2), 1073. <http://dx.doi.org/10.1086/423835>.
- Burlaga, L.F., Klein, L., Sheeley, Jr., N.R., Michels, D.J., Howard, R.A., Koomen, M.J., Schwenn, R., Rosenbauer, H., 1982. A magnetic cloud and a coronal mass ejection. *Geophys. Res. Lett.* 9 (12), 1317–1320. <http://dx.doi.org/10.1029/GL009i012p01317>, arXiv:<https://agupubs.onlinelibrary.wiley.com/doi/pdf/10.1029/GL009i012p01317> URL <https://agupubs.onlinelibrary.wiley.com/doi/abs/10.1029/GL009i012p01317>.
- Burlaga, L., Sittler, E., Mariani, F., Schwenn, a.R., 1981. Magnetic loop behind an interplanetary shock: Voyager, helios, and IMP 8 observations. *J. Geophys. Res. Space Phys.* 86 (A8), 6673–6684.
- Cameron, R., Schüssler, M., 2015. The crucial role of surface magnetic fields for the solar dynamo. *Science* 347 (6228), 1333–1335. <http://dx.doi.org/10.1126/science.1261470>, arXiv:<https://www.science.org/doi/pdf/10.1126/science.1261470> URL <https://www.science.org/doi/abs/10.1126/science.1261470>.
- Cane, H.V., Wibberenz, G., Richardson, I.G., von Rosenvinge, T.T., 1999. Cosmic ray modulation and the solar magnetic field. *Geophys. Res. Lett.* 26 (5), 565–568. <http://dx.doi.org/10.1029/1999GL900032>, arXiv:<https://agupubs.onlinelibrary.wiley.com/doi/pdf/10.1029/1999GL900032> URL <https://agupubs.onlinelibrary.wiley.com/doi/abs/10.1029/1999GL900032>.
- Chandrasekhar, S., 1961. Hydrodynamic and Hydromagnetic Stability.
- Charbonneau, P., 2020. Dynamo models of the solar cycle. *Living Rev. Sol. Phys.* 17 (1), 4.
- Charbonneau, P., Dikpati, M., 2008. Stochastic fluctuations in a Babcock-Leighton model of the solar cycle. *Astrophys. J.* 543, 1027. <http://dx.doi.org/10.1086/317142>.
- Chatterjee, P., Nandy, D., Choudhuri, A.R., 2004. Full-sphere simulations of a circulation-dominated solar dynamo: Exploring the parity issue. *Astron. Astrophys.* 427, 1019–1030. <http://dx.doi.org/10.1051/0004-6361:20041199>, arXiv:[astro-ph/0405027](https://astro-ph/0405027).
- Chen, P.F., 2011. Coronal mass ejections: Models and their observational basis. *Living Rev. Sol. Phys.* 8 (1), 1. <http://dx.doi.org/10.12942/lrsp-2011-1>.
- Chen, G.-m., Xu, J., Wang, W., Burns, A.G., 2014. A comparison of the effects of CIR- and CME-induced geomagnetic activity on thermospheric densities and spacecraft orbits: Statistical studies. *J. Geophys. Res. Space Phys.* 119 (9), 7928–7939.
- Chi, Y., Shen, C., Luo, B., Wang, Y., Xu, M., 2018. Geoeffectiveness of stream interaction regions from 1995 to 2016. *Space Weather* 16 (12), 1960–1971.
- Chou, D.-Y., Dai, D.-C., 2001. Solar cycle variations of subsurface meridional flows in the Sun. *Astrophys. J. Lett.* 559 (2), L175–L178. <http://dx.doi.org/10.1086/323724>.
- Christensen-Dalsgaard, J., 2002. Helioseismology. *Rev. Modern Phys.* 74, 1073–1129. <http://dx.doi.org/10.1103/RevModPhys.74.1073>, URL <https://link.aps.org/doi/10.1103/RevModPhys.74.1073>.
- Christon, S.P., Eastman, T.E., Doke, T., Frank, L.A., Gloeckler, G., Kojima, H., Kokubun, S., Lui, A.T.Y., Matsumoto, H., McEntire, R.W., Mukai, T., Nylund, S.R., Paterson, W.R., Roelof, E.C., Saito, Y., Sotirelis, T., Tsuruda, K., Williams, D.J., Yamamoto, T., 1998. Magnetospheric plasma regimes identified using geotail measurements: 2. statistics, spatial distribution, and geomagnetic dependence. *J. Geophys. Res. Space Phys.* 103 (A10), 23521–23542. <http://dx.doi.org/10.1029/98JA01914>, arXiv:<https://agupubs.onlinelibrary.wiley.com/doi/pdf/10.1029/98JA01914> URL <https://agupubs.onlinelibrary.wiley.com/doi/abs/10.1029/98JA01914>.
- Clette, F., Cliver, E., Lefèvre, L., Svalgaard, L., Vaquero, J., 2015. Revision of the sunspot number(s). *Space Weather* 13, <http://dx.doi.org/10.1002/2015SW001264>.
- Cook, G.R., Mackay, D.H., Nandy, D., 2009. Solar cycle variations of coronal null points: Implications for the magnetic breakout model of coronal mass ejections. *Astrophys. J.* 704 (2), 1021–1035. <http://dx.doi.org/10.1088/0004-637X/704/2/1021>.

- Cranmer, S.R., Winebarger, A.R., 2019. The properties of the solar corona and its connection to the solar wind. *Annu. Rev. Astron. Astrophys.* 57, 157–187. <http://dx.doi.org/10.1146/annurev-astro-091918-104416>, arXiv:1811.00461.
- Daglis, I.A., 2001. The storm-time ring current. *Space Sci. Rev.* 98 (3), 343–363. <http://dx.doi.org/10.1023/A:1013873329054>.
- Daglis, I.A., Chang, L.C., Dasso, S., Gopalswamy, N., Khabarova, O.V., Kilpuu, E., Lopez, R., Marsh, D., Mattthes, K., Nandy, D., Seppälä, A., Shiokawa, K., Thiéblemont, R., Zong, Q., 2021. Predictability of variable solar-terrestrial coupling. *Ann. Geophys.* 39 (6), 1013–1035. <http://dx.doi.org/10.5194/angeo-39-1013-2021>.
- Das, S.B., Basak, A., Nandy, D., Vaidya, B., 2019. Modeling star-planet interactions in far-out planetary and exoplanetary systems. *Astrophys. J.* 877 (2), 80. <http://dx.doi.org/10.3847/1538-4357/ab18ad>, arXiv:1812.07767.
- Dash, S., Bhowmik, P., Athira, B.S., Ghosh, N., Nandy, D., 2020a. Prediction of the Sun's coronal magnetic field and forward-modeled polarization characteristics for the 2019 July 2 total solar eclipse. *Astrophys. J.* 890 (1), 37. <http://dx.doi.org/10.3847/1538-4357/ab6a91>, arXiv:1906.10201.
- Dash, S., Bhowmik, P., Nandy, D., 2019. Prediction of the Sun's corona for the total solar eclipse on 2019 July 2. *Res. Notes Am. Astron. Soc.* 3 (6), 86. <http://dx.doi.org/10.3847/2515-5172/ab2ae3>.
- Dash, S., Nandy, D., Pal, S., 2020b. Dynamics of the Sun's polar field: Possible insights from out of the ecliptic observations. In: AGU Fall Meeting Abstracts, Vol. 2020. SH014–06.
- Dash, S., Nandy, D., Usoskin, I., 2022. Long-term forcing of sun's coronal field, open flux and cosmic ray modulation potential during grand minima, maxima and regular activity phases by the solar dynamo mechanism. arXiv e-prints arXiv:2208.12103.
- Dasso, S., Mandrini, C.H., Démoulin, P., Luoni, M.L., 2006. A new model-independent method to compute magnetic helicity in magnetic clouds. *Astron. Astrophys.* 455 (1), 349–359. <http://dx.doi.org/10.1051/0004-6361:20064806>.
- de Vries, H., 1958. Variation in concentration of radiocarbon with time and location on earth. *Proc. Koninkl. Nederl. Akad. Wetenschappen*, B 61, 1–9.
- Desai, M., Giacalone, J., 2016. Large gradual solar energetic particle events. *Living Rev. Sol. Phys.* 13 (1), 3. <http://dx.doi.org/10.1007/s41116-016-0002-5>.
- Dhuri, D.B., Hanasoge, S.M., Cheung, M.C.M., 2019. Machine learning reveals systematic accumulation of electric current in lead-up to solar flares. *Proc. Natl. Acad. Sci.* 116 (23), 11141–11146. <http://dx.doi.org/10.1073/pnas.1820244116>, arXiv:1905.10167.
- Dikpati, M., Charbonneau, P., 1999. A Babcock-Leighton flux transport dynamo with solar-like differential rotation. *Astrophys. J.* 518 (1), 508.
- Dong, C., Lee, Y., Ma, Y., Lingam, M., Bouger, S., Luhmann, J., Curry, S., Toth, G., Nagy, A., Tenishev, V., Fang, X., Mitchell, D., Brain, D., Jakovsky, B., 2018. Modeling martian atmospheric losses over time: Implications for exoplanetary climate evolution and habitability. *Astrophys. J. Lett.* 859 (1), L14. <http://dx.doi.org/10.3847/2041-8213/aac489>.
- D'Silva, S., Choudhuri, A.R., 1993. A theoretical model for tilts of bipolar magnetic regions. *Astron. Astrophys.* 272, 621.
- Dumbović, M., Čalogović, J., Vršnak, B., Temmer, M., Mays, M.L., Veronig, A., Piantschitsch, I., 2018. The drag-based ensemble model (DBEM) for coronal mass ejection propagation. *Astrophys. J.* 854 (2), 180.
- Durney, B.R., 1995. On a Babcock-Leighton dynamo model with a deep-seated generating layer for the toroidal magnetic field. *Sol. Phys.* 160 (2), 213–235.
- Duvall, Jr., T.L., Jefferies, S.M., Harvey, J.W., Pomerantz, M.A., 1993. Time-distance helioseismology. *Nature* 362 (6419), 430–432. <http://dx.doi.org/10.1038/362430a0>.
- Ebihara, Y., 2019. Simulation study of near-earth space disturbances: 1. magnetic storms. *Prog. Earth Planet. Sci.* 6 (1), 16. <http://dx.doi.org/10.1186/s40645-019-0264-3>.
- Eddy, J.A., 1976. The maunder minimum. *Science* 192 (4245), 1189–1202. <http://dx.doi.org/10.1126/science.192.4245.1189>, arXiv:https://www.science.org/doi/pdf/10.1126/science.192.4245.1189 URL https://www.science.org/doi/abs/10.1126/science.192.4245.1189.
- Egan, H., Jarvinen, R., Ma, Y., Brain, D., 2019. Planetary magnetic field control of ion escape from weakly magnetized planets. *Mon. Not. R. Astron. Soc.* 488 (2), 2108–2120. <http://dx.doi.org/10.1093/mnras/stz1819>, arXiv:https://academic.oup.com/mnras/article-pdf/488/2/2108/28967571/stz1819.pdf URL https://doi.org/10.1093/mnras/stz1819.
- Egeland, A., Burke, W.J., 2012. The ring current: a short biography. *Hist. Geo Space Sci.* 3 (2), 131–142. <http://dx.doi.org/10.5194/hgss-3-131-2012>, URL https://hgss.copernicus.org/articles/3/131/2012/.
- Fan, Y., Fisher, G.H., Deluca, E.E., 1993. The origin of morphological asymmetries in Bipolar Active Regions. *Astrophys. J.* 405, 390. <http://dx.doi.org/10.1086/172370>.
- Farrugia, C.J., Burlaga, L.F., Lepping, R.P., 1997. Magnetic clouds and the quiet-storm effect at Earth. In: Magnetic Storms. American Geophysical Union (AGU), pp. 91–106. <http://dx.doi.org/10.1029/GM098p0091>, arXiv:https://agupubs.onlinelibrary.wiley.com/doi/pdf/10.1029/GM098p0091 URL https://agupubs.onlinelibrary.wiley.com/doi/abs/10.1029/GM098p0091.
- Finley, A.J., Matt, S.P., See, V., 2018. The effect of magnetic variability on stellar angular momentum loss. I. the solar wind torque during sunspot cycles 23 and 24. *Astrophys. J.* 864 (2), 125. <http://dx.doi.org/10.3847/1538-4357/aad7b6>.
- Fisk, L.A., 1980. Solar modulation of galactic cosmic rays. In: Pepin, R.O., Eddy, J.A., Merrill, R.B. (Eds.), *The Ancient Sun: Fossil Record in the Earth, Moon and Meteorites*. pp. 103–118.
- Fisk, L.A., Schwadron, N.A., 2001. The behavior of the open magnetic field of the Sun. *Astrophys. J.* 560 (1), 425–438. <http://dx.doi.org/10.1086/322503>.
- Fletcher, L., Dennis, B.R., Hudson, H.S., Krucker, S., Phillips, K., Veronig, A., Battaglia, M., Bone, L., Caspi, A., Chen, Q., et al., 2011. An observational overview of solar flares. *Space Sci. Rev.* 159 (1), 19–106.
- Futaana, Y., Stenberg Wieser, G., Barabash, S., Luhmann, J.G., 2017. Solar wind interaction and impact on the Venus Atmosphere. *Space Sci. Rev.* 212 (3–4), 1453–1509. <http://dx.doi.org/10.1007/s11214-017-0362-8>.
- Gallet, F., Charbonnel, C., Amard, L., Brun, S., Palacios, A., Mathis, S., 2016. Impacts of stellar evolution and dynamics on the habitable zone: The role of rotation and magnetic activity. *Astron. Astrophys.* 597, <http://dx.doi.org/10.1051/0004-6361/201629034>.
- Garushkina, N., Jaynes, A., Liemohn, M., 2017. Space weather effects produced by the ring current particles. *Space Sci. Rev.* 212 (3), 1315–1344. <http://dx.doi.org/10.1007/s11214-017-0412-2>.
- Ghizaru, M., Charbonneau, P., Smolarkiewicz, P.K., 2010. Magnetic cycles in global large-eddy simulations of solar convection. *Astrophys. J. Lett.* 715 (2), L133. <http://dx.doi.org/10.1088/2041-8205/715/2/L133>.
- Gigolashvili, M.S., Japaridze, D.R., Mdzinarishvili, T.G., Chargeishvili, B.B., 2005. N S asymmetry in the solar differential rotation during 1957–1993. *Sol. Phys.* 227 (1), 27–38. <http://dx.doi.org/10.1007/s11207-005-1214-3>.
- Giles, P.M., 2000. Time-distance measurements of large-scale flows in the solar convection zone (Ph.D. thesis). Stanford University, California.
- Gizon, L., Duvall, Jr., T.L., Larsen, R.M., 2001. Probing surface flows and magnetic activity with time-distance helioseismology. In: Brekke, P., Fleck, B., Gurman, J.B. (Eds.), *Recent Insights Into the Physics of the Sun and Heliosphere: Highlights from SOHO and Other Space Missions*, Vol. 203. p. 189.
- Gleissberg, W., 1955. Der rhythmus der zonenwanderung der sonnenflecken. *Z. Naturforsch.* 37, 108.
- Gold, T., Hoyle, F., 1960. On the origin of solar flares. *Mon. Not. R. Astron. Soc.* 120 (2), 89–105. <http://dx.doi.org/10.1093/mnras/120.2.89>, arXiv:https://academic.oup.com/mnras/article-pdf/120/2/89/8074642/mnras120-0089.pdf URL https://doi.org/10.1093/mnras/120.2.89.
- Goldreich, P., Kumar, P., 1990. Wave generation by turbulent convection. *Astrophys. J.* 363, 694. <http://dx.doi.org/10.1086/169376>.
- Gopalswamy, N., 2007. Properties of interplanetary coronal mass ejections. In: *Solar Dynamics and Its Effects on the Heliosphere and Earth*. Springer New York, New York, NY, pp. 145–168. [http://dx.doi.org/10.1007/978-0-387-69532-7\\_11](http://dx.doi.org/10.1007/978-0-387-69532-7_11).
- Gopalswamy, N., 2011. Universal heliospherical processes. In: *The Sun, The Solar Wind, and The Heliosphere*. Springer, pp. 9–20.
- Gosling, J.T., 1990. Coronal mass ejections and magnetic flux ropes in interplanetary space. In: *Physics of Magnetic Flux Ropes*. American Geophysical Union (AGU), pp. 343–364. <http://dx.doi.org/10.1029/GM058p0343>, arXiv:https://agupubs.onlinelibrary.wiley.com/doi/pdf/10.1029/GM058p0343 URL https://agupubs.onlinelibrary.wiley.com/doi/abs/10.1029/GM058p0343.
- Gough, D.O., Kosovichev, A.G., Toomre, J., Anderson, E., Antia, H.M., Basu, S., Chaboyer, B., Chitre, S.M., Christensen-Dalsgaard, J., Dziembowski, W.A., Eff-Darwich, A., Elliott, J.R., Giles, P.M., Goode, P.R., Guzik, J.A., Harvey, J.W., Hill, F., Leibacher, J.W., Monteiro, M.J.P.F.G., Richard, O., Sekii, T., Shibahashi, H., Takata, M., Thompson, M.J., Vauclair, S., Vorontsov, S.V., 1996. The seismic structure of the Sun. *Science* 272 (5266), 1296–1300. <http://dx.doi.org/10.1126/science.272.5266.1296>, arXiv:https://www.science.org/doi/pdf/10.1126/science.272.5266.1296 URL https://www.science.org/doi/abs/10.1126/science.272.5266.1296.
- Guerrero, G., Dal Pino, E.D.G., 2008. Turbulent magnetic pumping in a Babcock-Leighton solar dynamo model. *Astron. Astrophys.* 485 (1), 267–273.
- Guerrero, G.A., Munoz, J., 2004. Kinematic solar dynamo models with a deep meridional flow. *Mon. Not. R. Astron. Soc.* 350 (1), 317–322.
- Gunell, H., Maggiolo, R., Nilsson, H., Stenberg Wieser, G., Slapak, R., Lindkvist, J., Hamrin, M., De Keyser, J., 2018. Why an intrinsic magnetic field does not protect a planet against atmospheric escape. *Astron. Astrophys.* 614, <http://dx.doi.org/10.1051/0004-6361/201832934>.
- Gupta, S., Basak, A., Nandy, D., 2023. Impact of changing stellar and planetary magnetic fields on (Exo)planetary environments and atmospheric mass loss. <http://dx.doi.org/10.48550/arXiv.2303.04770>, arXiv e-prints arXiv:2303.04770.
- Haber, D.A., Hindman, B.W., Toomre, J., Bogart, R.S., Larsen, R.M., Hill, F., 2002. Evolving submerged meridional circulation cells within the upper convection zone revealed by ring-diagram analysis. *Astrophys. J.* 570 (2), 855–864. <http://dx.doi.org/10.1086/339631>.
- Hale, G.E., 1913. Preliminary results of an attempt to detect the general magnetic field of the Sun. *Astrophys. J.* 38, 27.
- Hale, G.E., Ellerman, F., Nicholson, S.B., Joy, A.H., 1919. The magnetic polarity of sun-spots. *Astrophys. J.* 49, 153. <http://dx.doi.org/10.1086/142452>.
- Hanasoge, S.M., 2022. Surface and interior meridional circulation in the Sun. *Living Rev. Sol. Phys.* 19 (1), 3. <http://dx.doi.org/10.1007/s41116-022-00034-7>.
- Harbach, L.M., Moschou, S.P., Garraffo, C., Drake, J.J., Alvarado-Gómez, J.D., Cohen, O., Fraschetti, F., 2021. Stellar winds drive strong variations in exoplanet evaporative outflow patterns and transit absorption signatures. *Astrophys. J.* 913 (2), 130. <http://dx.doi.org/10.3847/1538-4357/abf63a>.

- Hassler, D.M., Gibson, S., Newmark, J.S., Featherstone, N.A., Upton, L., Vialli, N.M., Hoeksema, J.T., Auchere, F., Birch, A., Braun, D., Charbonneau, P., Colannino, R., DeForest, C., Dikpati, M., Downs, C., Duncan, N., Elliott, H.A., Fan, Y., Fineschi, S., Gizon, L., Gosain, S., Harra, L., Hindman, B., Berghmans, D., Lepri, S.T., Linker, J., Moldwin, M.B., Munoz-Jaramillo, A., Nandy, D., Rivera, Y., Schou, J., Sokol, J., Thompson, B., Velli, M., Woods, T.N., Zhao, J., 2023. Solaris: A focused solar polar discovery-class mission to achieve the highest priority heliophysics science now. <http://dx.doi.org/10.48550/arXiv.2301.07647>, arXiv e-prints arXiv:2301.07647.
- Hathaway, D.H., 1996. Doppler measurements of the Sun's meridional flow. *Astrophys. J.* 460, 1027. <http://dx.doi.org/10.1086/177029>.
- Hathaway, D.H., 2015. The solar cycle. *Living Rev. Sol. Phys.* 12 (1), 4.
- Hathaway, D.H., Gilman, P.A., Harvey, J.W., Hill, F., Howard, R.F., Jones, H.P., Kasher, J.C., Leibacher, J.W., Pintar, J.A., Simon, G.W., 1996. GONG observations of solar surface flows. *Science* 272 (5266), 1306–1309. <http://dx.doi.org/10.1126/science.272.5266.1306>, arXiv:<https://www.science.org/doi/pdf/10.1126/science.272.5266.1306> URL <https://www.science.org/doi/abs/10.1126/science.272.5266.1306>.
- Hathaway, D.H., Nandy, D., Wilson, R.M., Reichmann, E.J., 2003. Evidence that a deep meridional flow sets the sunspot cycle period. *Astrophys. J.* 589 (1), 665–670. <http://dx.doi.org/10.1086/374393>.
- Hayakawa, H., Owens, M.J., Lockwood, M., Sôma, M., 2020. The solar corona during the total eclipse on 1806 June 16: Graphical evidence of the coronal structure during the dalton minimum. *Astrophys. J.* 900 (2), 114. <http://dx.doi.org/10.3847/1538-4357/ab9807>, arXiv:2006.02868.
- Hazra, S., Brun, A.S., Nandy, D., 2020a. Does the mean-field  $\alpha$  effect have any impact on the memory of the solar cycle? *Astron. Astrophys.* 642, A51. <http://dx.doi.org/10.1051/0004-6361/201937287>, arXiv:2003.02776.
- Hazra, S., Cohen, O., Sokolov, I.V., 2022. Exoplanet radio transits as a probe for exoplanetary magnetic fields-time-dependent MHD simulations. *Astrophys. J.* 936 (2), 144. <http://dx.doi.org/10.3847/1538-4357/ac8978>, arXiv:2208.06006.
- Hazra, S., Nandy, D., 2016. A proposed paradigm for solar cycle dynamics mediated via turbulent pumping of magnetic flux in Babcock-Leighton-type solar dynamos. *Astrophys. J.* 832 (1), 9. <http://dx.doi.org/10.3847/0004-637X/832/1/9>, arXiv:1608.08167.
- Hazra, S., Nandy, D., 2019. The origin of parity changes in the solar cycle. *Mon. Not. R. Astron. Soc.* 489 (3), 4329–4337. <http://dx.doi.org/10.1093/mnras/stz2476>, arXiv:1906.06780.
- Hazra, G., Nandy, D., Kitchatinov, L., Choudhuri, A.R., 2023. Mean field models of flux transport dynamo and meridional circulation in the Sun and stars. <http://dx.doi.org/10.48550/arXiv.2302.09390>, arXiv e-prints arXiv:2302.09390.
- Hazra, S., Nandy, D., Ravindra, B., 2015. The relationship between solar coronal X-Ray brightness and active region magnetic fields: A study using high-resolution hinode observations. *Sol. Phys.* 290 (3), 771–785. <http://dx.doi.org/10.1007/s11207-015-0652-9>, arXiv:1406.1683.
- Hazra, S., Passos, D., Nandy, D., 2014. A stochastically forced time delay solar dynamo model: Self-consistent recovery from a maulder-like grand minimum necessitates a mean-field alpha effect. *Astrophys. J.* 789 (1), 5. <http://dx.doi.org/10.1088/0004-637X/789/1/5>, arXiv:1307.5751.
- Hazra, S., Sardar, G., Chowdhury, P., 2020b. Distinguishing between flaring and nonflaring active regions. *Astron. Astrophys.* 639, A44. <http://dx.doi.org/10.1051/0004-6361/201937426>.
- Heinemann, S.G., Temmer, M., Farrugia, C.J., Dissauer, K., Kay, C., Wiegelmann, T., Dumbović, M., Veronig, A.M., Podladchikova, T., Hofmeister, S.J., et al., 2019. CME-HSS interaction and characteristics tracked from Sun to Earth. *Sol. Phys.* 294 (9), 1–22.
- Hill, F., 1999. Ring-diagram analysis: Status and perspectives. In: SOHO-9 Workshop on Helioseismic Diagnostics of Solar Convection and Activity, Vol. 9, p. 2.
- Hotta, H., Kusano, K., 2021. Solar differential rotation reproduced with high-resolution simulation. *Nat. Astron.* 5 (11), 1100–1102. <http://dx.doi.org/10.1038/s41550-021-01459-0>.
- Hotta, H., Kusano, K., Shimada, R., 2022. Generation of solar-like differential rotation. *Astrophys. J.* 933 (2), 199. <http://dx.doi.org/10.3847/1538-4357/ac7395>.
- Hotta, H., Rempel, M., Yokoyama, T., 2016. Large-scale magnetic fields at high Reynolds numbers in magnetohydrodynamic simulations. *Science* 351 (6280), 1427–1430. <http://dx.doi.org/10.1126/science.aad1893>, arXiv:<https://www.science.org/doi/pdf/10.1126/science.aad1893> URL <https://www.science.org/doi/abs/10.1126/science.aad1893>.
- Howard, T.A., Harrison, R.A., 2013. Stealth coronal mass ejections: A perspective. *Sol. Phys.* 285 (1–2), 269–280. <http://dx.doi.org/10.1007/s11207-012-0217-0>.
- Howard, R., Labonte, B.J., 1980. The sun is observed to be a torsional oscillator with a period of 11 years. *Astrophys. J. Lett.* 239, L33–L36. <http://dx.doi.org/10.1086/183286>.
- Howe, R., Christensen-Dalsgaard, J., Hill, F., Komm, R.W., Larsen, R.M., Schou, J., Thompson, M.J., Toomre, J., 2000. Deeply penetrating banded zonal flows in the solar convection zone. *Astrophys. J. Lett.* 533 (2), L163–L166. <http://dx.doi.org/10.1086/312623>, arXiv:<https://arxiv.org/abs/astro-ph/0003121>.
- Hu, Q., Qiu, J., Dasgupta, B., Khare, A., Webb, G.M., 2014. Structures of interplanetary magnetic flux ropes and comparison with their solar sources. *Astrophys. J.* 793 (1), 53. <http://dx.doi.org/10.1088/0004-637X/793/1/53>.
- Huang, X., Wang, H., Xu, L., Liu, J., Li, R., Dai, X., 2018. Deep learning based solar flare forecasting model. I. Results for line-of-sight magnetograms. *Astrophys. J.* 856 (1), 7.
- Hudson, H.S., 1997. The solar antecedents of geomagnetic storms. In: Magnetic Storms. American Geophysical Union (AGU), pp. 35–44. <http://dx.doi.org/10.1029/GM098p0035>, arXiv:<https://agupubs.onlinelibrary.wiley.com/doi/pdf/10.1029/GM098p0035> URL <https://agupubs.onlinelibrary.wiley.com/doi/abs/10.1029/GM098p0035>.
- Hultqvist, B., Øieroset, M., Paschmann, G., Treumann, R.A., 1999. Source and loss processes in the magnetotail. In: Hultqvist, B., Øieroset, M., Paschmann, G., Treumann, R.A. (Eds.), Magnetospheric Plasma Sources and Losses: Final Report of the ISSI Study Project on Source and Loss Processes. Springer Netherlands, Dordrecht, pp. 285–353. [http://dx.doi.org/10.1007/978-94-011-4477-3\\_6](http://dx.doi.org/10.1007/978-94-011-4477-3_6).
- Iwai, K., Shiota, D., Tokumaru, M., Fujiki, K., Den, M., Kubo, Y., 2021. Validation of coronal mass ejection arrival-time forecasts by magnetohydrodynamic simulations based on interplanetary scintillation observations. *Earth Planets Space* 73 (1), 9. <http://dx.doi.org/10.1186/s40623-020-01345-5>.
- Iyemori, T., Takeda, M., Nose, M., Odagi, Y., Toh, H., 2009. Mid-latitude Geomagnetic Indices "ASY" and "SYM" for 2009 (Provisional). Data Analysis Center for Geomagnetism and Space Magnetism, Graduate School of Science, Kyoto University, Japan, URL <http://wdc.kugi.kyoto-u.ac.jp/aeasy/asym.pdf>.
- Jian, L., Russell, C., Luhmann, J., Skoug, R., 2006. Properties of stream interactions at one AU during 1995–2004. *Sol. Phys.* 239 (1), 337–392.
- Jiang, J., Cameron, R.H., Schmitt, D., Işık, E., 2013. Modeling solar cycles 15 to 21 using a flux transport dynamo. *Astron. Astrophys.* 553, A128. <http://dx.doi.org/10.1051/0004-6361/201321145>, arXiv:1304.5730.
- Jiang, J., Cameron, R.H., Schmitt, D., Schüssler, M., 2011. The solar magnetic field since 1700. I. Characteristics of sunspot group emergence and reconstruction of the butterfly diagram. *Astron. Astrophys.* 528, A82. <http://dx.doi.org/10.1051/0004-6361/201016167>, arXiv:1102.1266.
- Jiang, J., Hathaway, D.H., Cameron, R.H., Solanki, S.K., Gizon, L., Upton, L., 2014. Magnetic flux transport at the solar surface. *Space Sci. Rev.* 186 (1–4), 491–523. <http://dx.doi.org/10.1007/s11214-014-0083-1>, arXiv:1408.3186.
- Kallenrode, M.-B., 2001. The terrestrial magnetosphere. In: Space Physics: An Introduction to Plasmas and Particles in the Heliosphere and Magnetospheres. Springer Berlin Heidelberg, Berlin, Heidelberg, pp. 217–284. [http://dx.doi.org/10.1007/978-3-662-04443-8\\_8](http://dx.doi.org/10.1007/978-3-662-04443-8_8).
- Käpylä, P.J., Käpylä, M.J., Olspt, N., Warnecke, J., Brandenburg, A., 2017. Convection-driven spherical shell dynamos at varying Prandtl numbers. *Astron. Astrophys.* 599, A4. <http://dx.doi.org/10.1051/0004-6361/201628973>, URL <https://doi.org/10.1051/0004-6361/201628973>.
- Karak, B.B., Choudhuri, A.R., 2011. The Waldmeier effect and the flux transport solar dynamo. *Mon. Not. R. Astron. Soc.* 410 (3), 1503–1512. <http://dx.doi.org/10.1111/j.1365-2966.2010.17531.x>, arXiv:1008.0824.
- Karak, B.B., Miesch, M., 2017. Solar cycle variability induced by tilt angle scatter in a Babcock-Leighton solar dynamo model. *Astrophys. J.* 847 (1), 69. <http://dx.doi.org/10.3847/1538-4357/aa8636>.
- Karak, B.B., Nandy, D., 2012. Turbulent pumping of magnetic flux reduces solar cycle memory and thus impacts predictability of the Sun's activity. *Astrophys. J. Lett.* 761 (1), L13. <http://dx.doi.org/10.1088/2041-8205/761/1/L13>, arXiv:1206.2106.
- Kay, C., Gopalswamy, N., 2017. Using the coronal evolution to successfully forward model CMEs' in situ magnetic profiles. *J. Geophys. Res. Space Phys.* 122 (12), 11–810.
- Kilpua, E., Koskinen, H.E.J., Pulkkinen, T.I., 2017. Coronal mass ejections and their sheath regions in interplanetary space. *Living Rev. Sol. Phys.* 14 (1), 5. <http://dx.doi.org/10.1007/s41116-017-0009-6>.
- Kilpua, E., Koskinen, H.E.J., Pulkkinen, T.I., 2017. Coronal mass ejections and their sheath regions in interplanetary space. *Living Rev. Sol. Phys.* 14 (1), 5. <http://dx.doi.org/10.1007/s41116-017-0009-6>.
- Knobloch, E., Tobias, S., Weiss, N., 1998. Modulation and symmetry changes in stellar dynamos. *Mon. Not. R. Astron. Soc.* 297 (4), 1123–1138.
- Koskinen, H.E.J., Huttunen, K.E.J., 2006. Space weather: from solar eruptions to magnetospheric storms. In: Solar Eruptions and Energetic Particles. American Geophysical Union (AGU), pp. 375–385. <http://dx.doi.org/10.1002/9781118666203.ch34>, arXiv:<https://agupubs.onlinelibrary.wiley.com/doi/pdf/10.1002/9781118666203.ch34> URL <https://agupubs.onlinelibrary.wiley.com/doi/abs/10.1002/9781118666203.ch34>.
- Koskinen, H.E.J., Huttunen, K.E.J., 2007. Geoeffectivity of coronal mass ejections. In: Baker, D.N., Klecker, B., Schwartz, S.J., Schwenn, R., Von Steiger, R. (Eds.), Solar Dynamics and Its Effects on the Heliosphere and Earth. Springer New York, New York, NY, pp. 169–181. [http://dx.doi.org/10.1007/978-0-387-69532-7\\_12](http://dx.doi.org/10.1007/978-0-387-69532-7_12).
- Kumar, R., Jouve, L., Nandy, D., 2019. A 3D kinematic babcock leighton solar dynamo model sustained by dynamic magnetic buoyancy and flux transport processes. *Astron. Astrophys.* 623, A54. <http://dx.doi.org/10.1051/0004-6361/201834705>, arXiv:1901.04251.
- Kusano, K., Iju, T., Bamba, Y., Inoue, S., 2020. A physics-based method that can predict imminent large solar flares. *Science* 369 (6503), 587–591. <http://dx.doi.org/10.1126/science.aaz2511>, arXiv:<https://www.science.org/doi/pdf/10.1126/science.aaz2511> URL <https://www.science.org/doi/abs/10.1126/science.aaz2511>.

- Lakhina, G.S., Tsurutani, B.T., 2016. Geomagnetic storms: historical perspective to modern view. *Geosci. Lett.* 3 (1), 1–11.
- Lammer, H., Güdel, M., Kulikov, Y., Ribas, I., Zaqrashvili, T., Khodachenko, M., Kislyakova, K., Gröller, H., Odert, P., Leitzinger, M., Fichtinger, B., Krauss, S., Hausleitner, W., Holmström, M., Sanz-Forcada, J., Lichtenegger, H., Hanslmeier, A., Shematovich, V., Bisikalo, D., Fridlund, M., 2012. Variability of solar/stellar activity and magnetic field and its influence on planetary atmosphere evolution. *Earth Planets Space* 64, 179–199. <http://dx.doi.org/10.5047/eps.2011.04.002>.
- Le, G., Russell, C.T., Takahashi, K., 2004. Morphology of the ring current derived from magnetic field observations. *Ann. Geophys.* 22 (4), 1267–1295. <http://dx.doi.org/10.5194/angeo-22-1267-2004>, URL <https://angeo.copernicus.org/articles/22/1267/2004/>.
- Lee, E.H., Ahn, Y.S., Yang, H.J., Chen, K.Y., 2004. The sunspot and auroral activity cycle derived from Korean historical records of the 11th–18th century. *Sol. Phys.* 224 (1), 373–386. <http://dx.doi.org/10.1007/s11207-005-5199-8>.
- Leighton, R.B., 1969. A magneto-kinematic model of the solar cycle. *Astrophys. J.* 156, 1. <http://dx.doi.org/10.1086/149943>.
- Leighton, R.B., Noyes, R.W., Simon, G.W., 1962. Velocity fields in the solar atmosphere. I. Preliminary report. *Astrophys. J.* 135, 474. <http://dx.doi.org/10.1086/147285>.
- Leka, K., Barnes, G., 2003. Photospheric magnetic field properties of flaring versus flare-quiet active regions. II. Discriminant analysis. *Astrophys. J.* 595 (2), 1296.
- Lekshmi, B., Nandy, D., Antia, H.M., 2018. Asymmetry in solar torsional oscillation and the sunspot cycle. *Astrophys. J.* 861 (2), 121. <http://dx.doi.org/10.3847/1538-4357/aacbd5>, arXiv:1807.03588.
- Lekshmi, B., Nandy, D., Antia, H.M., 2019. Hemispheric asymmetry in meridional flow and the sunspot cycle. *Mon. Not. R. Astron. Soc.* 489 (1), 714–722. <http://dx.doi.org/10.1093/mnras/stz2168>.
- Lepri, S., Zurbuchen, T., 2010. Direct observational evidence of filament material within interplanetary coronal mass ejections. *Astrophys. J. Lett.* 723 (1), L22.
- Liu, W., Fujimoto, M. (Eds.), 2011. The Dynamic Magnetosphere, first ed. Springer, Dordrecht, <http://dx.doi.org/10.1007/978-94-007-0501-2>.
- Liu, L., Wang, Y., Liu, R., Zhou, Z., Temmer, M., Thalmann, J.K., Liu, J., Liu, K., Shen, C., Zhang, Q., Veronig, A.M., 2017. The causes of quasi-homologous CMEs. *Astrophys. J.* 844 (2), 141. <http://dx.doi.org/10.3847/1538-4357/aa7d56>.
- Liu, L., Wang, Y., Zhou, Z., Cui, J., 2021. The source locations of major flares and CMEs in Emerging Active Regions. *Astrophys. J.* 909 (2), 142. <http://dx.doi.org/10.3847/1538-4357/abde37>.
- Lu, J.Y., Liu, Z.Q., Kabin, K., Jing, H., Zhao, M.X., Wang, Y., 2013. The IMF dependence of the magnetopause from global MHD simulations. *J. Geophys. Res. Space Phys.* 118 (6), 3113–3125. <http://dx.doi.org/10.1002/jgra.50324>.
- Lugaz, N., Temmer, M., Wang, Y., Farrugia, C.J., 2017. The interaction of successive coronal mass ejections: A review. *Sol. Phys.* 292 (4), 64. <http://dx.doi.org/10.1007/s11207-017-1091-6>, URL <https://doi.org/10.1007/s11207-017-1091-6>.
- Luhmann, J.G., Gosling, J.T., Hoeksema, J.T., Zhao, X., 1998. The relationship between large-scale solar magnetic field evolution and coronal mass ejections. *JGRA* 103, 6585. <http://dx.doi.org/10.1029/97JA03727>.
- Luhmann, J., Zhang, T., Petrinec, S., Russell, C., Gazis, P., Barnes, A., 1993. Solar cycle 21 effects on the interplanetary magnetic field and related parameters at 0.7 and 1.0 AU. *J. Geophys. Res.: Atmos.* 98, <http://dx.doi.org/10.1029/92JA02235>.
- Mackay, D.H., Yeates, A.R., 2012. The Sun's global photospheric and coronal magnetic fields: Observations and models. *Living Rev. Sol. Phys.* 9 (1), 6. <http://dx.doi.org/10.12942/lrsp-2012-6>, arXiv:1211.6545.
- Maltsev, Y.P., 2004. Points of controversy in the study of magnetic storms. *Space Sci. Rev.* 110 (3), 227–267. <http://dx.doi.org/10.1023/B:SPAC.0000023410.77752.30>.
- Manchester, IV, W.B., Gombosi, T.I., Roussev, I., De Zeeuw, D.L., Sokolov, I., Powell, K.G., Tóth, G., Opher, M., 2004. Three-dimensional MHD simulation of a flux rope driven CME. *J. Geophys. Res. Space Phys.* 109 (A1).
- Manoharan, P.K., Gopalswamy, N., Yashiro, S., Lara, A., Michalek, G., Howard, R.A., 2004. Influence of coronal mass ejection interaction on propagation of interplanetary shocks. *J. Geophys. Res. Space Phys.* 109 (A6), <http://dx.doi.org/10.1029/2003JA010300>, arXiv:<https://agupubs.onlinelibrary.wiley.com/doi/pdf/10.1029/2003JA010300> URL <https://agupubs.onlinelibrary.wiley.com/doi/abs/10.1029/2003JA010300>.
- Martin-Belda, D., Cameron, R.H., 2016. Surface flux transport simulations: Effect of inflows toward active regions and random velocities on the evolution of the Sun's large-scale magnetic field. *Astron. Astrophys.* 586, A73. <http://dx.doi.org/10.1051/0004-6361/201527213>, arXiv:1512.02541.
- Mazumder, R., 2019. Properties of filaments in solar cycle 20–23 from McIntosh archive. *Res. Astron. Astrophys.* 19 (6), 080. <http://dx.doi.org/10.1088/1674-4527/19/6/80>.
- Mazumder, R., Bhowmik, P., Nandy, D., 2018. The association of filaments, polarity inversion lines, and coronal hole properties with the sunspot cycle: An analysis of the mcintosh database. *Astrophys. J.* 868 (1), 52. <http://dx.doi.org/10.3847/1538-4357/aae68a>, arXiv:1810.02133.
- Mazumder, R., Chatterjee, S., Nandy, D., Banerjee, D., 2021. Solar cycle evolution of filaments over a century: Investigations with the meudon and McIntosh hand-drawn archives. *Astrophys. J.* 919 (2), 125. <http://dx.doi.org/10.3847/1538-4357/ac09f6>, arXiv:2106.04320.
- Menvielle, M., Iyemori, T., Marchaudon, A., Nosé, M., 2011. Geomagnetic indices. In: Mandea, M., Korte, M. (Eds.), *Geomagnetic Observations and Models*. Springer Netherlands, Dordrecht, pp. 183–228. [http://dx.doi.org/10.1007/978-94-481-9858-0\\_8](http://dx.doi.org/10.1007/978-94-481-9858-0_8).
- Miesch, M.S., Teweldebirhan, K., 2016. A three-dimensional Babcock–Leighton solar dynamo model: Initial results with axisymmetric flows. *Adv. Space Res.* 58 (8), 1571–1588. <http://dx.doi.org/10.1016/j.asr.2016.02.018>, URL <https://www.sciencedirect.com/science/article/pii/S0273117716001198> Solar Dynamo Frontiers.
- Mignone, A., Bodo, G., Massaglia, S., Matsakos, T., Tesileanu, O., Zanni, C., Ferrari, A., 2007. PLUTO: A numerical code for computational astrophysics. *Astrophys. J. Suppl. Ser.* 170 (1), 228–242. <http://dx.doi.org/10.1086/513316>.
- Mikić, Z., Downs, C., Linker, J.A., Caplan, R.M., Mackay, D.H., Upton, L.A., Riley, P., Lionello, R., Török, T., Titov, V.S., Wijaya, J., Druckmüller, M., Pasachoff, J.M., Carlos, W., 2018. Predicting the corona for the 21 August 2017 total solar eclipse. *Nat. Astron.* 2, 913–921. <http://dx.doi.org/10.1038/s41550-018-0562-5>.
- Moon, Y.J., Chae, J., Wang, H., Park, Y., 2003. Magnetic helicity change rate associated with three X-class eruptive flares. *Adv. Space Res.* 32 (10), 1953–1958. [http://dx.doi.org/10.1016/S0273-1177\(03\)90632-6](http://dx.doi.org/10.1016/S0273-1177(03)90632-6), URL <https://www.sciencedirect.com/science/article/pii/S0273117703906326>.
- Möstl, C., Amerstorfer, T., Palmerio, E., Isavnin, A., Farrugia, C.J., Lowder, C., Winslow, R.M., Donnerer, J.M., Kilpua, E.K., Boakes, P.D., 2018. Forward modeling of coronal mass ejection flux ropes in the inner heliosphere with 3DCORE. *Space Weather* 16 (3), 216–229.
- Muñoz-Jaramillo, A., Nandy, D., Martens, P.C.H., 2009. Helioseismic data inclusion in solar dynamo models. *Astrophys. J.* 698 (1), 461–478. <http://dx.doi.org/10.1088/0004-637X/698/1/461>, arXiv:0811.3441.
- Muñoz-Jaramillo, A., Nandy, D., Martens, P.C.H., 2011. Magnetic quenching of turbulent diffusivity: Reconciling mixing-length theory estimates with kinematic dynamo models of the solar cycle. *Astrophys. J. Lett.* 727 (1), L23. <http://dx.doi.org/10.1088/2041-8205/727/1/L23>, arXiv:1007.1262.
- Muñoz-Jaramillo, A., Nandy, D., Martens, P.C.H., Yeates, A.R., 2010. A double-ring algorithm for modeling Solar Active Regions: Unifying kinematic dynamo models and surface flux-transport simulations. *Astrophys. J. Lett.* 720 (1), L20–L25. <http://dx.doi.org/10.1088/2041-8205/720/1/L20>, arXiv:1006.4346.
- Muñoz-Jaramillo, A., Sheeley, N.R., Zhang, J., DeLuca, E.E., 2012. Calibrating 100 years of polar faculae measurements: Implications for the evolution of the heliospheric magnetic field. *Astrophys. J.* 753 (2), 146. <http://dx.doi.org/10.1088/0004-637X/753/2/146>, arXiv:1303.0345.
- Muñoz-Jaramillo, A., Nandy, D., Martens, P.C., 2009. Helioseismic data inclusion in solar dynamo models. *Astrophys. J.* 698 (1), 461.
- Munoz-Jaramillo, A., Nandy, D., Martens, P.C., Yeates, A.R., 2010. A double-ring algorithm for modeling solar active regions: unifying kinematic dynamo models and surface flux-transport simulations. *Astrophys. J. Lett.* 720 (1), L20.
- Mursula, K., Manoharan, P., Nandy, D., Tanskainen, E., Verronen, P., 2013. Long-term solar activity and its implications to the heliosphere, geomagnetic activity, and the Earth's climate. Preface to the special issue on space climate. *J. Space Weather Space Clim.* 3, A21. <http://dx.doi.org/10.1051/swsc/2013043>.
- Nagy, M., Lemerle, A., Labouville, F., Petrovay, K., Charbonneau, P., 2017. The effect of “Rogue” active regions on the solar cycle. *Sol. Phys.* 292 (11), 167. <http://dx.doi.org/10.1007/s11207-017-1194-0>, arXiv:1712.02185.
- Nakamura, R., Kokubun, S., Mukai, T., Yamamoto, T., 1997. Changes in the distant tail configuration during geomagnetic storms. *J. Geophys. Res. Space Phys.* 102 (A5), 9587–9601. <http://dx.doi.org/10.1029/97JA00095>, arXiv: <https://agupubs.onlinelibrary.wiley.com/doi/pdf/10.1029/97JA00095> URL <https://agupubs.onlinelibrary.wiley.com/doi/abs/10.1029/97JA00095>.
- Nandy, D., 2002. Constraints on the solar internal magnetic field from a buoyancy driven solar dynamo. *Astrophys. Space Sci.* 282 (1), 209–219. <http://dx.doi.org/10.1023/A:1021632522168>.
- Nandy, D., 2004. Exploring magnetic activity from The Sun to the Stars. *Sol. Phys.* 224 (1–2), 161–169. <http://dx.doi.org/10.1007/s11207-005-4990-x>.
- Nandy, D., 2006. Magnetic helicity and flux tube dynamics in the solar convection zone: Comparisons between observation and theory. *J. Geophys. Res.* 111 (A12), A12S01. <http://dx.doi.org/10.1029/2006JA011882>.
- Nandy, D., 2021. Progress in solar cycle predictions: Sunspot cycles 24–25 in perspective. *Sol. Phys.* 296 (3), 54. <http://dx.doi.org/10.1007/s11207-021-01797-2>, arXiv:2009.01908.
- Nandy, D., Banerjee, D., Bhowmik, P., Brun, A.S., Cameron, R.H., Gibson, S.E., Hanasoge, S., Harra, L., Hassler, D.M., Jain, R., Jiang, J., Jouve, L., Mackay, D.H., Mahajan, S.S., Mandrini, C.H., Owens, M., Pal, S., Pinto, R.F., Saha, C., Sun, X., Tripathi, D., Usoskin, I.G., 2023. Exploring the solar poles: The last great frontier of the sun. <http://dx.doi.org/10.48550/ARXIV.2301.00010>, arXiv URL <https://arxiv.org/abs/2301.00010>.
- Nandy, D., Bhowmik, P., Yeates, A.R., Panda, S., Tarafder, R., Dash, S., 2018. The large-scale coronal structure of the 2017 August 21 great American eclipse: An assessment of solar surface flux transport model enabled predictions and observations. *Astrophys. J.* 853 (1), 72. <http://dx.doi.org/10.3847/1538-4357/aaa1eb>.
- Nandy, D., Choudhuri, A.R., 2001. Toward a mean field formulation of the Babcock–Leighton type solar dynamo. I.  $\alpha$ -coefficient versus Durney's Double-Ring approach. *Astrophys. J.* 551 (1), 576–585. <http://dx.doi.org/10.1086/320057>, arXiv:astro-ph/0107466.

- Nandy, D., Choudhuri, A.R., 2002. Explaining the latitudinal distribution of sunspots with deep meridional flow. *Science* 296 (5573), 1671–1673. <http://dx.doi.org/10.1126/science.1070955>.
- Nandy, D., Martens, P.C.H., 2007. Space climate and the solar stellar connection: What can we learn from the stars about long-term solar variability? *Adv. Space Res.* 40 (7), 891–898. <http://dx.doi.org/10.1016/j.asr.2007.01.079>.
- Nandy, D., Martens, P.C.H., Obrido, V., Dash, S., Georgieva, K., 2021. Solar evolution and extrema: current state of understanding of long-term solar variability and its planetary impacts. *Prog. Earth Planet. Sci.* 8 (1), 40. <http://dx.doi.org/10.1186/s40645-021-00430-x>.
- Nandy, D., Muñoz-Jaramillo, A., Martens, P.C.H., 2011. The unusual minimum of sunspot cycle 23 caused by meridional plasma flow variations. *Nature* 471 (7336), 80–82. <http://dx.doi.org/10.1038/nature09786>, arXiv:1303.0349.
- Nelson, N.J., Brown, B.P., Brun, A.S., Miesch, M.S., Toomre, J., 2012. Magnetic wreaths and cycles in convective dynamos. *Astrophys. J.* 762 (2), 73. <http://dx.doi.org/10.1088/0004-637X/762/2/73>.
- Nitta, N.V., Mulligan, T., Kilpua, E.K., Lynch, B.J., Mierla, M., O’Kane, J., Pagano, P., Palmerio, E., Pomoell, J., Richardson, I.G., et al., 2021. Understanding the origins of problem geomagnetic storms associated with “stealth” coronal mass ejections. *Space Sci. Rev.* 217 (8), 1–53.
- Nose, M., Iyemori, T., Sugiura, M., Kamei, T., 2015. Geomagnetic Dst Index. World Data Center for Geomagnetism, <http://dx.doi.org/10.17593/14515-74000>.
- Owens, M.J., Cargill, P.J., Pagel, C., Siscoe, G.L., Crooker, N.U., 2005. Characteristic magnetic field and speed properties of interplanetary coronal mass ejections and their sheath regions. *J. Geophys. Res. Space Phys.* 110 (A1), <http://dx.doi.org/10.1029/2004JA010814>, arXiv:<https://agupubs.onlinelibrary.wiley.com/doi/pdf/10.1029/2004JA010814> URL <https://agupubs.onlinelibrary.wiley.com/doi/abs/10.1029/2004JA010814>.
- Owens, M.J., Crooker, N.U., 2006. Coronal mass ejections and magnetic flux buildup in the heliosphere. *JGRA* 111, <http://dx.doi.org/10.1029/2006JA011641>.
- Owens, M.J., Forsyth, R.J., 2013. The heliospheric magnetic field. *Living Rev. Sol. Phys.* 10 (1), 5. <http://dx.doi.org/10.12942/lrsp-2013-5>.
- Pal, S., 2022. Uncovering the process that transports magnetic helicity to coronal mass ejection flux ropes. *Adv. Space Res.* 70 (6), 1601–1613. <http://dx.doi.org/10.1016/j.asr.2021.11.013>.
- Pal, S., Bhowmik, P., Mahajan, S.S., Nandy, D., 2023. Impact of anomalous active regions on the large-scale magnetic field of the sun. arXiv e-prints <http://dx.doi.org/10.48550/arXiv.2305.13145>.
- Pal, S., Dash, S., Nandy, D., 2020. Flux erosion of magnetic clouds by reconnection with the sun’s open flux. *Geophys. Res. Lett.* 47 (8), e86372. <http://dx.doi.org/10.1029/2019GL086372>, arXiv:2103.05990.
- Pal, S., Gopalswamy, N., Nandy, D., Akiyama, S., Yashiro, S., Makela, P., Xie, H., 2017. A sun-to-earth analysis of magnetic helicity of the 2013 March 17–18 interplanetary coronal mass ejection. *Astrophys. J.* 851 (2), 123. <http://dx.doi.org/10.3847/1538-4357/aa9983>, arXiv:1712.01114.
- Pal, S., Kilpua, E., Good, S., Pomoell, J., Price, D.J., 2021a. Uncovering erosion effects on magnetic flux rope twist. *Astron. Astrophys.* 650, A176. <http://dx.doi.org/10.1051/0004-6361/202040070>, arXiv:2104.03569.
- Pal, S., Lynch, B.J., Good, S.W., Palmerio, E., Asvestari, E., Pomoell, J., Stevens, M.L., Kilpua, E.K.J., 2022a. Eruption and interplanetary evolution of a stealthy streamer-blowout CME observed by PSP at 0.5 AU. *Front. Astron. Space Sci.* 9, <http://dx.doi.org/10.3389/fspas.2022.903676>, URL <https://www.frontiersin.org/articles/10.3389/fspas.2022.903676>.
- Pal, S., Nandy, D., Kilpua, E.K.J., 2022b. Magnetic cloud prediction model for forecasting space weather relevant properties of earth-directed coronal mass ejections. *Astron. Astrophys.* 665, A110. <http://dx.doi.org/10.1051/0004-6361/202243513>.
- Pal, S., Nandy, D., Srivastava, N., Gopalswamy, N., Panda, S., 2018. Dependence of coronal mass ejection properties on their solar source active region characteristics and associated flare reconnection flux. *Astrophys. J.* 865 (1), 4. <http://dx.doi.org/10.3847/1538-4357/aa1a10>, arXiv:1808.04144.
- Palmerio, E., Kay, C., Al-Haddad, N., Lynch, B.J., Yu, W., Stevens, M.L., Pal, S., Lee, C.O., 2021. Predicting the magnetic fields of a stealth CME detected by parker solar probe at 0.5 au. *Astrophys. J.* 920 (2), 65. <http://dx.doi.org/10.3847/1538-4357/ac25f4>, arXiv:2109.04933.
- Palmerio, E., Nitta, N.V., Mulligan, T., Mierla, M., O’Kane, J., Richardson, I.G., Sinha, S., Srivastava, N., Yardley, S.L., Zhukov, A.N., 2021. Investigating remote-sensing techniques to reveal stealth coronal mass ejections. *Front. Astron. Space Sci.* 109.
- Parker, E.N., 1955a. The formation of sunspots from the solar toroidal field. *Astrophys. J.* 121, 491.
- Parker, E.N., 1955b. Hydromagnetic dynamo models. *Astrophys. J.* 122, 293.
- Parker, E.N., 1957. Newtonian development of the dynamical properties of ionized gases of low density. *Phys. Rev.* 107, 924–933. <http://dx.doi.org/10.1103/PhysRev.107.924>.
- Parker, E.N., 1958. Dynamics of the interplanetary gas and magnetic fields. *Astrophys. J.* 128, 664. <http://dx.doi.org/10.1086/146579>.
- Pasachoff, J.M., Lockwood, C., Meadors, E., Yu, R., Perez, C., Peñaloza-Murillo, M.A., Seaton, D.B., Voulgaris, A., Dantowitz, R., Rušin, V., Economou, T., 2018. Images and spectra of the 2017 total solar eclipse corona from our oregon site. *Front. Astron. Space Sci.* 5, 37. <http://dx.doi.org/10.3389/fspas.2018.00037>.
- Passos, D., Nandy, D., Hazra, S., Lopes, I., 2014. A solar dynamo model driven by mean-field alpha and Babcock-Leighton sources: fluctuations, grand-minima-maxima, and hemispheric asymmetry in sunspot cycles. *Astron. Astrophys.* 563, A18. <http://dx.doi.org/10.1051/0004-6361/201322635>, arXiv:1309.2186.
- Petrie, G.J.D., 2015. Solar magnetism in the polar regions. *Living Rev. Sol. Phys.* 12 (1), 5. <http://dx.doi.org/10.1007/lrsp-2015-5>.
- Petrovay, K., 2020. Solar cycle prediction. *Living Rev. Sol. Phys.* 17 (1), 2. <http://dx.doi.org/10.1007/s41116-020-0022-z>, arXiv:1907.02107.
- Potgieter, M.S., 2013. Solar modulation of cosmic rays. *Living Rev. Sol. Phys.* 10 (1), 3. <http://dx.doi.org/10.12942/lrsp-2013-3>, arXiv:1306.4421.
- Proctor, M.R.E., Weiss, N.O., 1982. REVIEW ARTICLE: Magnetohydrodynamics. *Rep. Progr. Phys.* 45 (11), 1317–1379. <http://dx.doi.org/10.1088/0034-4885/45/11/003>.
- Pudovkin, M.I., Besser, B.P., Zaitseva, S.A., 1998. Magnetopause stand-off distance in dependence on the magnetosheath and solar wind parameters. *Ann. Geophys.* 16 (4), 388–396. <http://dx.doi.org/10.1007/s00585-998-0388-z>, URL <https://angeo.copernicus.org/articles/16/388/1998/>.
- Rastatter, L., Kuznetsova, M.M., Glocer, A., Welling, D., Meng, X., Raeder, J., Wilberger, M., Jordanova, V.K., Yu, Y., Zaharia, S., Weigel, R.S., Saizykin, S., Boynton, R., Wei, H., Eccles, V., Horton, W., Mays, M.L., Gannon, J., 2013. Geospace environment modeling 2008–2009 challenge: Dst index. *Space Weather* 11 (4), 187–205. <http://dx.doi.org/10.1002/swe.20036>, arXiv: <https://agupubs.onlinelibrary.wiley.com/doi/pdf/10.1002/swe.20036> URL <https://agupubs.onlinelibrary.wiley.com/doi/abs/10.1002/swe.20036>.
- Robbrecht, E., Patsourakos, S., Vourlidas, A., 2009. No trace left behind: STEREO observation of a coronal mass ejection without low coronal signatures. *Astrophys. J.* 701 (1), 283–291. <http://dx.doi.org/10.1088/0004-637X/701/1/283>, arXiv:0905.2583.
- Roy, S., Nandy, D., 2021a. Magnetohydrodynamical understanding of the interactions between coronal mass ejections and earth’s magnetosphere. *Earth Space Sci. Open Arch.* 18. <http://dx.doi.org/10.1002/essoar.10505902.1>.
- Roy, S., Nandy, D., 2021b. Modelling the impact of magnetic storms on planetary environments. In: EGU General Assembly Conference Abstracts. pp. EGU21–8863. <http://dx.doi.org/10.5194/egusphere-egu21-8863>.
- Roy, S., Nandy, D., 2022. A time-efficient, data driven modelling approach to predict the geomagnetic impact of coronal mass ejections. arXiv e-prints arXiv:2210.00071.
- Ruffenach, A., Lavraud, B., Farrugia, C.J., Démoulin, P., Dasso, S., Owens, M.J., Sauvad, J.-A., Rouillard, A.P., Lynnyk, A., Foullon, C., Savani, N.P., Luhmann, J.G., Galvin, A.B., 2015. Statistical study of magnetic cloud erosion by magnetic reconnection. *J. Geophys. Res. Space Phys.* 120 (1), 43–60. <http://dx.doi.org/10.1002/2014JA020628>, arXiv:<https://agupubs.onlinelibrary.wiley.com/doi/pdf/10.1002/2014JA020628> URL <https://agupubs.onlinelibrary.wiley.com/doi/abs/10.1002/2014JA020628>.
- Saha, C., Chandra, S., Nandy, D., 2022. Evidence of persistence of weak magnetic cycles driven by meridional plasma flows during solar grand minima phases. *Mon. Not. R. Astron. Soc.* 517 (1), L36–L40. <http://dx.doi.org/10.1093/mnrasl/slac104>, arXiv:2209.14651.
- Sakai, S., Seki, K., Terada, N., Shinagawa, H., Tanaka, T., Ebihara, Y., 2018. Effects of a weak intrinsic magnetic field on atmospheric escape from Mars. *Geophys. Res. Lett.* 45 (18), 9336–9343. <http://dx.doi.org/10.1029/2018gl079972>.
- Sakata, R., Seki, K., Sakai, S., Terada, N., Shinagawa, H., Tanaka, T., 2020. Effects of an intrinsic magnetic field on ion loss from ancient Mars based on multispecies MHD simulations. *J. Geophys. Res. Space Phys.* 125 (2), <http://dx.doi.org/10.1029/2019ja026945>.
- Sarkar, R., Gopalswamy, N., Srivastava, N., 2020. An observationally constrained analytical model for predicting the magnetic field vectors of interplanetary coronal mass ejections at 1 au. *Astrophys. J.* 888 (2), 121.
- Savani, N.P., Vourlidas, A., Szabo, A., Mays, M.L., Richardson, I., Thompson, B., Pulkkinen, A., Evans, R., Nieves-Chinchilla, T., 2015. Predicting the magnetic vectors within coronal mass ejections arriving at Earth: 1. Initial architecture. *Space Weather* 13 (6), 374–385.
- Scherrer, P.H., Schou, J., Bush, R.I., Kosovichev, A.G., Bogart, R.S., Hoeksema, J.T., Liu, Y., Duvall, T.L., Zhao, J., Title, A.M., Schrijver, C.J., Tarbell, T.D., Tomczyk, S., 2012. The helioseismic and magnetic imager (HMI) investigation for the solar dynamics observatory (SDO). *Sol. Phys.* 275 (1–2), 207–227. <http://dx.doi.org/10.1007/s11207-011-9834-2>.
- Schillings, A., Slapak, R., Nilsson, H., Yamauchi, M., Dandouras, I., Westerberg, L.G., 2019. Earth atmospheric loss through the plasma mantle and its dependence on solar wind parameters. *Earth Planets Space* 71 (1), <http://dx.doi.org/10.1186/s40623-019-1048-0>.
- Schrijver, C.J., DeRosa, M.L., 2003. Photospheric and heliospheric magnetic fields. *Sol. Phys.* 212 (1), 165–200. <http://dx.doi.org/10.1023/A:1022908504100>.
- Schrijver, C.J., Kauristie, K., Aylward, A.D., Denardini, C.M., Gibson, S.E., Glover, A., Gopalswamy, N., Grande, M., Hapgood, M., Heynderickx, D., Jakowski, N., Kalegaev, V.V., Lapenta, G., Linker, J.A., Liu, S., Mandrini, C.H., Mann, I.R., Nagatsuma, T., Nandy, D., Obara, T., Paul O’Brien, T., Onsager, T., Opgenoorth, H.J., Terkildsen, M., Valladares, C.E., Vilmer, N., 2015. Understanding space weather to shield society: A global road map for 2015–2025 commissioned by COSPAR and ILWS. *Adv. Space Res.* 55 (12), 2745–2807. <http://dx.doi.org/10.1016/j.asr.2015.03.023>, arXiv:1503.06135.

- Schwabe, H., 1844. Schreiben des herrn professors plantamour, directors der sternwarte in genf, an den herausgeber. Astron. Nachr. 21 (15), 233–234. <http://dx.doi.org/10.1002/asna.18440211504>, arXiv:<https://agupubs.onlinelibrary.wiley.com/doi/pdf/10.1002/asna.18440211504> URL <https://agupubs.onlinelibrary.wiley.com/doi/abs/10.1002/asna.18440211504>.
- Schwartz, S.J., 1985. Solar wind and the earth's bow shock. In: Priest, E.R. (Ed.), *Solar System Magnetic Fields*. Springer Netherlands, Dordrecht, pp. 190–223. [http://dx.doi.org/10.1007/978-94-009-5482-3\\_8](http://dx.doi.org/10.1007/978-94-009-5482-3_8).
- Schwenn, R., 2006. Space weather: The solar perspective. *Living Rev. Sol. Phys.* 3 (1), 1–72.
- Schwenn, R., Marsch, E. (Eds.), 1991a. *Physics of the Inner Heliosphere II - Particles, Waves and Turbulence*, first ed. Springer, Berlin, Heidelberg. <http://dx.doi.org/10.1007/978-3-642-75364-0>.
- Schwenn, R., Marsch, E. (Eds.), 1991b. *Physics of the Inner Heliosphere I - Large-Scale Phenomena*, first ed. Springer, Berlin, Heidelberg. <http://dx.doi.org/10.1007/978-3-642-75361-9>.
- Scolini, C., Chané, E., Temmer, M., Kilpua, E.K., Dissauer, K., Veronig, A.M., Palmeiro, E., Pomoelli, J., Dumbović, M., Guo, J., et al., 2020. CME–CME interactions as sources of CME geoeffectiveness: The formation of the complex ejecta and intense geomagnetic storm in 2017 early September. *Astrophys. J. Suppl. Ser.* 247 (1), 21.
- See, V., Jardine, M., Vidotto, A.A., Petit, P., Marsden, S.C., Jeffers, S.V., do Nascimento, J.D., 2014. The effects of stellar winds on the magnetospheres and potential habitability of exoplanets. *Astron. Astrophys.* 570, <http://dx.doi.org/10.1051/0004-6361/201424323>.
- Shen, C., Chi, Y., Wang, Y., Xu, M., Wang, S., 2017. Statistical comparison of the ICME's geoeffectiveness of different types and different solar phases from 1995 to 2014. *J. Geophys. Res. Space Phys.* 122 (6), 5931–5948. <http://dx.doi.org/10.1002/2016JA023768>, arXiv:[https://agupubs.onlinelibrary.wiley.com/doi/abs/10.1002/2016JA023768](https://agupubs.onlinelibrary.wiley.com/doi/pdf/10.1002/2016JA023768).
- Shen, F., Shen, C., Zhang, J., Hess, P., Wang, Y., Feng, X., Cheng, H., Yang, Y., 2014. Evolution of the 12 July 2012 CME from the Sun to the Earth: Data-constrained three-dimensional MHD simulations. *J. Geophys. Res. Space Phys.* 119 (9), 7128–7141.
- Shen, C., Wang, Y., Wang, S., Liu, Y., Liu, R., Vourlidas, A., Miao, B., Ye, P., Liu, J., Zhou, Z., 2012. Super-elastic collision of large-scale magnetized plasmoids in the heliosphere. *Nat. Phys.* 8 (12), 923–928. <http://dx.doi.org/10.1038/nphys2440>.
- Shen, C., Xu, M., Wang, Y., Chi, Y., Luo, B., 2018. Why the shock-ICME complex structure is important: Learning from the early 2017 September CMEs. *Astrophys. J.* 861 (1), 28. <http://dx.doi.org/10.3847/1538-4357/aac204>.
- Shibata, K., Magara, T., 2011. Solar flares: Magnetohydrodynamic processes. *Living Rev. Sol. Phys.* 8 (1), 6. <http://dx.doi.org/10.12942/lrsp-2011-6>.
- Shue, J.H., Chao, J.K., 2013. The role of enhanced thermal pressure in the earthward motion of the Earth's magnetopause. *J. Geophys. Res. Space Phys.* 118 (6), 3017–3026. <http://dx.doi.org/10.1002/jgra.50290>.
- Sinha, S., Gupta, O., Singh, V., Lekshmi, B., Nandy, D., Mitra, D., Chatterjee, S., Bhattacharya, S., Chatterjee, S., Srivastava, N., Brandenburg, A., Pal, S., 2022. A comparative analysis of machine-learning models for solar flare forecasting: Identifying high-performing active region flare indicators. *Astrophys. J.* 935 (1), 45. <http://dx.doi.org/10.3847/1538-4357/ac7955>, arXiv:2204.05910.
- Sinha, S., Srivastava, N., Nandy, D., 2019. Solar filament eruptions as precursors to flare-CME events: Establishing the temporal connection. *Astrophys. J.* 880 (2), 84. <http://dx.doi.org/10.3847/1538-4357/ab2239>.
- Snodgrass, H.B., 1983. Magnetic rotation of the solar photosphere. *Astrophys. J.* 270, 288–299. <http://dx.doi.org/10.1086/161121>.
- Solanki, S.K., 1993. Smallscale solar magnetic fields - an overview. *Space Sci. Rev.* 63 (1–2), 1–188. <http://dx.doi.org/10.1007/BF00749277>.
- Song, H., Tan, C., Jing, J., Wang, H., Yurchyshyn, V., Abramenco, V., 2009. Statistical assessment of photospheric magnetic features in imminent solar flare predictions. *Sol. Phys.* 254 (1), 101–125.
- Spina, L., Nordlander, T., Casey, A.R., Bedell, M., D'Orazi, V., Meléndez, J., Karakas, A.I., Desidera, S., Baratella, M., Galarza, J.J.Y., Casali, G., 2020. How magnetic activity alters what we learn from stellar spectra. *Astrophys. J.* 895 (1), 52. <http://dx.doi.org/10.3847/1538-4357/ab8bd7>.
- St. Cyr, O.C., Plunkett, S.P., Michels, D.J., Paswaters, S.E., Koomen, M.J., Simnett, G.M., Thompson, B.J., Gurman, J.B., Schwenn, R., Webb, D.F., Hildner, E., Lamy, P.L., 2000. Properties of coronal mass ejections: SOHO LASCO observations from January 1996 to June 1998. *J. Geophys. Res.* 105 (A8), 18169–18186. <http://dx.doi.org/10.1029/1999JA000381>.
- Sterling, A.C., Moore, R.L., 2005. Slow-rise and fast-rise phases of an erupting solar filament, and flare emission onset. *Astrophys. J.* 630 (2), 1148.
- Suess, H.E., 1965. Secular variations of the cosmic-ray-produced carbon 14 in the atmosphere and their interpretations. *J. Geophys. Res.* (1896–1977) 70 (23), 5937–5952. <http://dx.doi.org/10.1029/JZ070i023p05937>, arXiv:[https://agupubs.onlinelibrary.wiley.com/doi/abs/10.1029/JZ070i023p05937](https://agupubs.onlinelibrary.wiley.com/doi/pdf/10.1029/JZ070i023p05937).
- Sugiura, M., 1964. Hourly values of equatorial dst for the IGY. Annals of the International Geophysical Year, Vol. 35. Pergamon Press, Oxford, URL [http://isgi.unistra.fr/Documents/References/Sugiura\\_AIGY\\_1964.pdf](http://isgi.unistra.fr/Documents/References/Sugiura_AIGY_1964.pdf).
- Sugiura, M., Kamei, T., 1991. Equatorial dst INDEX 1957–1986. International Union of Geodesy and Geophysics Association of Geomagnetism and Aeronomy (IAGA) Bulletin Number 40. ISGI PUBLICATIONS OFFICE, FRANCE, URL [http://isgi.unistra.fr/IAGABulletins/IAGA\\_Bulletin\\_40\\_Sugiura\\_Kamei\\_1991.pdf](http://isgi.unistra.fr/IAGABulletins/IAGA_Bulletin_40_Sugiura_Kamei_1991.pdf) URL <http://wdc.kugi.kyoto-u.ac.jp/dstdir/dst2/onDstindex.html>.
- Sung, S.K., Marubashi, K., Cho, K.S., Kim, Y.H., Kim, K.H., Chae, J., Moon, Y.J., Kim, I.H., 2009. A comparison of the initial speed of coronal mass ejections with the magnetic flux and magnetic helicity of magnetic clouds. *Astrophys. J.* 699 (1), 298.
- Temmer, M., Veronig, A., Peinhart, V., Vršnak, B., 2014. Asymmetry in the CME–CME interaction process for the events from 2011 February 14–15. *Astrophys. J.* 785 (2), 85.
- Thernisien, A., Howard, R., Vourlidas, A., 2006. Modeling of flux rope coronal mass ejections. *Astrophys. J.* 652 (1), 763.
- Toriumi, S., Wang, H., 2019. Flare-productive active regions. *Living Rev. Sol. Phys.* 16 (1), 3. <http://dx.doi.org/10.1007/s41116-019-0019-7>, arXiv:1904.12027.
- Tripathi, B., Nandy, D., Banerjee, S., 2021. Stellar mid-life crisis: subcritical magnetic dynamos of solar-like stars and the breakdown of gyrochronology. *Mon. Not. R. Astron. Soc.* 506 (1), L50–L54. <http://dx.doi.org/10.1093/mnrasl/slab035>, arXiv:1812.05533.
- Tripathi, D., Ramaprakash, A.N., Khan, A., Ghosh, A., Chatterjee, S., Banerjee, D., Chordia, P., Gandorfer, A., Krivova, N., Nandy, D., Rajarshi, C., Solanki, S.K., 2017. The solar ultraviolet imaging telescope on-board aditya-L1. *Current Sci.* 113 (04), 616. <http://dx.doi.org/10.18520/cs/v113/i04/616-619>.
- Upton, L., Hathaway, D.H., 2013. Predicting the sun's polar magnetic fields with a surface flux transport model. *Astrophys. J.* 780 (1), 5. <http://dx.doi.org/10.1088/0004-637X/780/1/5>.
- Usoskin, I.G., 2017. A history of solar activity over millennia. *Living Rev. Sol. Phys.* 14 (1), 3. <http://dx.doi.org/10.1007/s41116-017-0006-9>.
- Usoskin, I.G., Schüssler, M., Solanki, S.K., Mursula, K., 2005. Solar activity, cosmic rays, and Earth's temperature: A millennium-scale comparison. *J. Geophys. Res.* 110 (A10), A10102. <http://dx.doi.org/10.1029/2004JA010946>.
- van Ballegooijen, A.A., Cartledge, N.P., Priest, E.R., 1998. Magnetic flux transport and the formation of filament channels on the sun. *Astrophys. J.* 501 (2), 866–881. <http://dx.doi.org/10.1086/305823>.
- Vasiliev, S.S., Dergachev, V.A., 2002. The 2400-year cycle in atmospheric radiocarbon concentration: bispectrum of  $^{14}\text{C}$  data over the last 8000 years. *Ann. Geophys.* 20 (1), 115–120. <http://dx.doi.org/10.5194/angeo-20-115-2002>.
- Vidotto, A.A., 2021. The evolution of the solar wind. *Living Rev. Sol. Phys.* 18 (1), 3. <http://dx.doi.org/10.1007/s41116-021-00029-w>, arXiv:2103.15748.
- Vidotto, A.A., Cleary, A., 2020. Stellar wind effects on the atmospheres of close-in giants: a possible reduction in escape instead of increased erosion. *Mon. Not. R. Astron. Soc.* 494 (2), 2417–2428. <http://dx.doi.org/10.1093/mnras/staa852>, arXiv:<https://academic.oup.com/mnras/article-pdf/494/2/2417/33108649/staa852.pdf> URL <https://doi.org/10.1093/mnras/staa852>.
- Vidotto, A., Donati, J., Jardine, M., See, V., Petit, P., Boisse, I., Boro Saikia, S., Hebrard, E., Jeffers, S., Marsden, S., Morin, J., 2015. Could a change in magnetic field geometry cause the break in the wind-activity relation? *Mon. Not. R. Astron. Soc.* 455, 455. <http://dx.doi.org/10.1093/mnrasl/slv147>.
- Walker, R., Richard, R., Ogino, T., Ashour-Abdalla, M., 1999. The response of the magnetotail to changes in the IMF orientation: The magnetotail's long memory. *Phys. Chem. Earth C Sol. Terr. Planet. Sci.* 24 (1), 221–227. [http://dx.doi.org/10.1016/S1464-1917\(98\)00032-4](http://dx.doi.org/10.1016/S1464-1917(98)00032-4), URL <https://www.sciencedirect.com/science/article/pii/S1464191798000324> International Symposium on Solar-Terrestrial Coupling Processes.
- Wang, Y., Chen, C., Gui, B., Shen, C., Ye, P., Wang, S., 2011. Statistical study of coronal mass ejection source locations: Understanding CMEs viewed in coronagraphs. *J. Geophys. Res. Space Phys.* 116 (A4), <http://dx.doi.org/10.1029/2010JA016101>, arXiv:[https://agupubs.onlinelibrary.wiley.com/doi/abs/10.1029/2010JA016101](https://agupubs.onlinelibrary.wiley.com/doi/pdf/10.1029/2010JA016101) URL <https://agupubs.onlinelibrary.wiley.com/doi/abs/10.1029/2010JA016101>.
- Wang, Y., Guo, J., Li, G., Rousos, E., Zhao, J., 2022. Variation in cosmic-ray intensity lags sunspot number: Implications of late opening of solar magnetic field. *Astrophys. J.* 928 (2), 157. <http://dx.doi.org/10.3847/1538-4357/ac5896>.
- Wang, Y.M., Hawley, S.H., Sheeley, N.R., 1996. The magnetic nature of coronal holes. *Sci.* 271, 464. <http://dx.doi.org/10.1126/science.271.5248.464>.
- Wang, Y., Liu, L., Shen, C., Liu, R., Ye, P., Wang, S., 2013. Waiting times of quasi-homologous coronal mass ejections from super active regions. *Astrophys. J. Lett.* 763 (2), L43. <http://dx.doi.org/10.1088/2041-8205/763/2/L43>.
- Wang, Y., Shen, C., Liu, R., Liu, J., Guo, J., Li, X., Xu, M., Hu, Q., Zhang, T., 2018. Understanding the twist distribution inside magnetic flux ropes by atomizing an interplanetary magnetic cloud. *J. Geophys. Res. Space Phys.* 123 (5), 3238–3261. <http://dx.doi.org/10.1002/2017JA024971>, arXiv:[https://agupubs.onlinelibrary.wiley.com/doi/abs/10.1002/2017JA024971](https://agupubs.onlinelibrary.wiley.com/doi/pdf/10.1002/2017JA024971) URL <https://agupubs.onlinelibrary.wiley.com/doi/abs/10.1002/2017JA024971>.
- Wang, Y., Shen, C.L., Wang, S., Ye, P.Z., 2003. An empirical formula relating the geomagnetic storm's intensity to the interplanetary parameters:  $(-VB_z)$  and  $(\delta)$ . *Geophys. Res. Lett.* 30 (20), <http://dx.doi.org/10.1029/2003GL017901>, arXiv:[https://agupubs.onlinelibrary.wiley.com/doi/abs/10.1029/2003GL017901](https://agupubs.onlinelibrary.wiley.com/doi/pdf/10.1029/2003GL017901) URL <https://agupubs.onlinelibrary.wiley.com/doi/abs/10.1029/2003GL017901>.

- Wang, Y., Ye, P., Wang, S., Zhou, G., Wang, J., 2002. A statistical study on the geoeffectiveness of Earth-directed coronal mass ejections from March 1997 to December 2000. *J. Geophys. Res. Space Phys.* 107 (A11), SSH-2.
- Wang, Y., Zhang, J., 2007. A comparative study between eruptive X-Class flares associated with coronal mass ejections and confined X-Class flares. *Astrophys. J.* 665 (2), 1428. <http://dx.doi.org/10.1086/519765>.
- Wang, Y., Zhuang, B., Hu, Q., Liu, R., Shen, C., Chi, Y., 2016. On the twists of interplanetary magnetic flux ropes observed at 1 AU. *J. Geophys. Res. Space Phys.* 121 (10), 9316–9339. <http://dx.doi.org/10.1002/2016JA023075>, arXiv:<https://agupubs.onlinelibrary.wiley.com/doi/pdf/10.1002/2016JA023075> URL <https://agupubs.onlinelibrary.wiley.com/doi/abs/10.1002/2016JA023075>.
- Wanliss, J.A., Showalter, K.M., 2006. High-resolution global storm index: Dst versus SYM-H. *J. Geophys. Res. Space Phys.* 111 (A2), <http://dx.doi.org/10.1029/2005JA011034>, arXiv:<https://agupubs.onlinelibrary.wiley.com/doi/pdf/10.1029/2005JA011034> URL <https://agupubs.onlinelibrary.wiley.com/doi/abs/10.1029/2005JA011034>.
- Webb, D.F., 1995. Coronal mass ejections: The key to major interplanetary and geomagnetic disturbances. *Rev. Geophys.* 33 (S1), 577–583. <http://dx.doi.org/10.1029/95RG00345>, arXiv:<https://agupubs.onlinelibrary.wiley.com/doi/pdf/10.1029/95RG00345> URL <https://agupubs.onlinelibrary.wiley.com/doi/abs/10.1029/95RG00345>.
- Weiss, N., Tobias, S., 2016. Supermodulation of the Sun's magnetic activity: the effects of symmetry changes. *Mon. Not. R. Astron. Soc.* 456 (3), 2654–2661.
- Williams, D.J., 1983. The Earth's ring current: Causes, generation, and decay. In: Roederer, J.G. (Ed.), *Progress in Solar-Terrestrial Physics: Fifth International Symposium*. Ottawa, Canada, May 1982, Springer Netherlands, Dordrecht, pp. 223–234. [http://dx.doi.org/10.1007/978-94-009-7096-0\\_17](http://dx.doi.org/10.1007/978-94-009-7096-0_17).
- Wilmot-Smith, A.L., Martens, P.C.H., Nandy, D., Priest, E.R., Tobias, S.M., 2005. Low-order stellar dynamo models. *Mon. Not. R. Astron. Soc.* 363 (4), 1167–1172. <http://dx.doi.org/10.1111/j.1365-2966.2005.09514.x>.
- Wilmot-Smith, A.L., Nandy, D., Hornig, G., Martens, P.C.H., 2006. A time delay model for solar and stellar dynamos. *Astrophys. J.* 652 (1), 696–708. <http://dx.doi.org/10.1086/508013>.
- Wolf, M., 1852. Solar spots, on the periodic return of the. *Mon. Not. R. Astron. Soc.* 13, 29.
- Woodard, M.F., 2002. Inferring inhomogeneous structure in the sun directly from correlations in the seismic signal. In: *American Astronomical Society Meeting Abstracts #200*, Vol. 200. p. 89.02.
- Wu, C.J., Usoskin, I.G., Krivova, N., Kovaltsov, G.A., Baroni, M., Bard, E., Solanki, S.K., 2018. Solar activity over nine millennia: A consistent multi-proxy reconstruction. *Astron. Astrophys.* 615, A93. <http://dx.doi.org/10.1051/0004-6361/201731892>.
- Xu, M., Shen, C., Wang, Y., Luo, B., Chi, Y., 2019. Importance of shock compression in enhancing ICME's geoeffectiveness. *Astrophys. J. Lett.* 884 (2), L30. <http://dx.doi.org/10.3847/2041-8213/ab4717>.
- Yeates, A.R., 2020. How good is the bipolar approximation of active regions for surface flux transport? *Sol. Phys.* 295 (9), 119. <http://dx.doi.org/10.1007/s11207-020-01688-y>, arXiv:2008.03203.
- Yeates, A.R., Baker, D., van Driel-Gesztelyi, L., 2015. Source of a prominent poleward surge during solar cycle 24. *Sol. Phys.* 290 (11), 3189–3201. <http://dx.doi.org/10.1007/s11207-015-0660-9>, arXiv:1502.04854.
- Yeates, A.R., Bhowmik, P., 2022. Automated driving for global nonpotential simulations of the solar corona. *Astrophys. J.* 935 (1), 13. <http://dx.doi.org/10.3847/1538-4357/ac7de4>.
- Yeates, A., Muñoz-Jaramillo, A., 2013. Kinematic active region formation in a three-dimensional solar dynamo model. *Mon. Not. R. Astron. Soc.* 436 (4), 3366–3379.
- Yeates, A.R., Nandy, D., Mackay, D.H., 2008. Exploring the physical basis of solar cycle predictions: Flux transport dynamics and persistence of memory in advection-versus diffusion-dominated solar convection zones. *Astrophys. J.* 673 (1), 544–556. <http://dx.doi.org/10.1086/524352>, arXiv:0709.1046.
- Young, C.A., 1896. The Sun. D. Appleton and company, New York, URL <http://catalog.hathitrust.org/Record/001476804> 363 p..
- Yu, D., Huang, X., Wang, H., Cui, Y., 2009. Short-term solar flare prediction using a sequential supervised learning method. *Sol. Phys.* 255 (1), 91–105.
- Yuan, Y., Shih, F.Y., Jing, J., Wang, H.M., 2010. Automated flare forecasting using a statistical learning technique. *Res. Astron. Astrophys.* 10 (8), 785.
- Zhang, J., Temmer, M., Gopalswamy, N., Malandraki, O., Nitta, N.V., Patsourakos, S., Shen, F., Vršnak, B., Wang, Y., Webb, D., Desai, M.I., Dissauer, K., Dresing, N., Dumbović, M., Feng, X., Heinemann, S.G., Laurena, M., Lugaz, N., Zhuang, B., 2021. Earth-affecting solar transients: a review of progresses in solar cycle 24. *Prog. Earth Planet. Sci.* 8 (1), 56. <http://dx.doi.org/10.1186/s40645-021-00426-7>.
- Zhao, J., Kosovichev, A.G., 2004. Torsional oscillation, meridional flows, and vorticity inferred in the upper convection zone of the Sun by time-distance helioseismology. *Astrophys. J.* 603 (2), 776–784. <http://dx.doi.org/10.1086/381489>.
- Zurbuchen, T.H., Richardson, I.G., 2006. In-situ solar wind and magnetic field signatures of interplanetary coronal mass ejections. *Space Sci. Rev.* 123 (1), 31–43. <http://dx.doi.org/10.1007/s11214-006-9010-4>.